Reproductive Toxicology 33 (2012) 35–44

Contents lists available at SciVerse ScienceDirect

Reproductive Toxicology

journal homepage: www.elsevier.com/locate/reprotox

Involvement of gonadotropins in the induction of hypertrophy-hyperplasia in the interstitial tissues of ovaries in neonatally diethylstilbestrol-treated mice☆

Hanako Kakuta[a], Masami Tanaka[b], Pierre Chambon[c], Hajime Watanabe[d], Taisen Iguchi[d], Tomomi Sato[a,*]

[a] International Graduate School of Arts and Sciences, Yokohama City University, Yokohama 236-0027, Japan
[b] Department of Pharmacology, St. Marianna University School of Medicine, Kawasaki 216-8511, Japan
[c] Institut de Génétique et de Biologie Moléculaire et Cellulaire, CNRS/INSERM/ULP, Collége de France, BP163, 67404 Illkirch Cedex, France
[d] The Graduate University for Advanced Studies and Okazaki Institute for Integrative Bioscience, National Institute for Basic Biology, National Institutes of Natural Sciences, Okazaki 444-8787, Japan

ARTICLE INFO

Article history:
Received 13 May 2011
Received in revised form 2 October 2011
Accepted 24 October 2011
Available online 12 November 2011

Keywords:
Ovary
DES
Steroidogenesis
Interstitial cells

ABSTRACT

Neonatally diethylstilbestrol (DES) treatment causes hypertrophy-hyperplasia in the interstitial tissue of mouse ovaries. To understand the induction mechanism of the hypertrophy, mRNA expression involved in steroidogenesis in the ovary of neonatally DES-treated mice was examined. The expression of *StAR* and *Cyp11a1* was significantly reduced while *Cyp19* and *Sf-1* were stimulated in the ovary of neonatally DES-treated 3-month-old mice. Expression of those genes was not different between DES- and oil-treated mice after the gonadotropins treatment. *Lhb* in the pituitary of 3-month-old neonatally DES-treated mice was significantly decreased. Finally, ovaries from DES-treated mice transplanted to neonatally oil-treated hosts had developing follicles at several stages and corpora lutea, whereas grafted ovaries from neonatally oil-treated mice in 3-month-old neonatally DES-treated hosts showed lipid accumulation in the interstitial tissue. Thus, hypertrophy and accumulation of lipid droplets in interstitial cells of neonatally DES-treated mice is caused by impaired steroidogenesis due to the alterations of gonadotropins levels.

1. Introduction

Diethylstilbestrol (DES), a synthetic estrogen, had been prescribed for preventing abortion, however, women who were exposed to DES *in utero* developed vaginal clear-cell adenocarcinoma [1]. In mice, perinatal exposure to natural or synthetic estrogens, including DES, results in reproductive abnormalities such as absence of corpora lutea (CL), hypertrophy-hyperplasia of interstitial tissues, induction of polyovular follicles in the ovary and persistent vaginal cornification [2–6].

Hypertrophy-hyperplasia of interstitial tissues is already found in the ovary of 3-month-old prenatally DES-exposed mice, and a dramatic increase in lipid droplets in the interstitial tissue as determined by Oil Red O stain [3]. In a study of estrogen receptor α knockout (αERKO) mice, it was shown that the induction of hypertrophy-hyperplasia of interstitial tissues was mediated by ERα [7]. The absence of CL in the ovary of neonatally DES-treated mice is caused by lack of a luteinizing hormone (LH) surge [8–10]. In addition, plasma levels of testosterone (T) in neonatally DES-treated mice are lower than those in the controls, and ovariectomy, adrenalectomy or a combination of both surgeries shows no effect [11]. These results suggest that alterations in the hypothalamic–pituitary–gonadal (HPG) axis may affect steroidogenesis in the interstitial and theca cells of neonatally DES-treated mouse ovaries.

Several studies have shown that disruption of genes involved in steroidogenesis results in alterations of steroid levels and progressive increases in lipid deposits with age [12–14]. In theca and interstitial cells, cholesterol obtained from plasma lipoproteins is transferred by steroidogenic acute regulating (StAR) protein from the outer mitochondrial membrane to the inner membrane where cytochrome P450 side-chain cleaving enzyme (CYP11A1) is located [15,16]. CYP11A1 converts cholesterol to pregnenolone [15,16]. Ovaries from 8-week-old *Star* knockout (KO) mice retain a few scattered follicles and are largely composed of vacuolated stromal cells that stain with Oil Red O [12,13]. In addition, ovaries of *Cyp11a1* KO mice treated with daily injections of corticosteroids are similar to

☆ *Grant support*: This work was partially supported by a Grant-in-Aid for Scientific Research (B) (T.I.) from the Ministry of Education, Culture, Sports, Science and Technology of Japan, Grants for Strategic Research Projects at Yokohama City University (Nos. K19020, K2109, G2201 and W18005 to T.S.), a Health Sciences Research Grant from the Ministry of Health, Labor and Welfare, Japan (T.I.), and a Grant for Support of the Collaborative Study at NIBB (T.S).

* Corresponding author at: Graduate School of Nanobiosciences, Yokohama City University, 22-2 Seto, Kanazawa-ku, Yokohama 236-0027, Japan.
Tel.: +81 45 787 2394; fax: +81 45 787 2413.
E-mail address: tomomi@yokohama-cu.ac.jp (T. Sato).

0890-6238/$ – see front matter © 2011 Elsevier Inc. All rights reserved.
doi:10.1016/j.reprotox.2011.10.013

those of wild-type (WT) mice during the neonatal period, however, lipid accumulation is increased in interstitial cells around follicles at 13 days of age [14]. These results suggest that the failure of steroidogenesis leads to lipid accumulation in interstitial cells with age. Pregnenolone is converted to progesterone by 3β-hydroxysteroid dehydrogenase (3β-HSD) and/or dehydroepiandrosterone by C17-hydroxylase (CYP17A1) and then converted to androstendione by CYP17A1 and/or 3β-HSD, respectively [15,16]. Androstenedione synthesized in theca cells diffuses to granulosa cells and it is converted to T by 17β-hydroxysteroid dehydrogenase (17β-HSD) or estrone by aromatase (CYP19) and then 17β-estradiol (E2) by 17β-HSD [15,16]. Steroidogenesis is tightly regulated by the HPG axis. In theca and interstitial cells, androstenedione is produced for supplying androgen for granulosa cells to synthesize E2 in response to LH. Follicle stimulating hormone (FSH) is required for preantral to later-stage follicle development [17]. FSH also regulates the expression of CYP19 [18,19] in developing follicles where FSH receptors are located. The LH surge down-regulates this FSH-induced increase in *Cyp19* expression [20] and triggers ovulatory changes in the preovulatory follicle, including luteinization of the granulosa and theca cells and production of progesterone following the expression of *Star* and *Cyp11a1* [21,22].

The orphan nuclear receptors SF-1 and LRH-1 regulate critical genes in the reproductive axis and steroidogenesis [23,24]. In the ovary, SF-1 is localized in theca, interstitial and granulosa cells [23,25,26] and activates promoters of *Star*, *Cyp11a1*, *Cyp11b1* and *Cyp21* [27,28], through the consensus T/CAAGGTCA sequence. LH reduces SF-1 expression in preovulatory granulosa cells [29]. Granulosa-specific KO mice of *Sf-1* are infertile and show hemorrhagic cysts (HC) and the absence of CL in the ovary [30] similar to the phenotype of αERKO or *Cyp19* KO mice, suggesting that *Sf-1*KO mice have the defect in the synthesis of estrogen in the ovary. LRH-1 is mainly localized in granulosa cells and CLs, and regulates *Cyp19* [23]. Mice lacking *Lrh-1* in granulosa cells are sterile due to anovulation [31]. Lack of *Lrh-1* also results in an increase of intrafollicular E2 levels with elevated *Cyp19*, and decreases of *Star* and *Cyp11a1* in granulosa cells. These results suggest that SF-1 and LRH-1 have critical roles in the ovary. Since both SF-1 and LRH-1 are expressed in granulosa cells and have similar actions [24,32], distinct differences between the actions of SF-1 and LRH-1 within the ovary are still unclear [33].

In the present study, we aimed to identify the timing of lipid droplets accumulation in interstitial cells and examined the mRNA expression involved in steroidogenesis in the ovary of neonatally DES-treated mice. We hypothesized that the altered HPG axis caused the lipid accumulation in the ovary of neonatally DES-treated mice. Therefore, ovaries from neonatally DES-treated mice were grafted under the renal capsule of ovariectomized neonatally oil-treated mice and vice versa was also examined. In addition, the serum levels of E2 in neonatally oil- and DES-treated mice were measured to assess steroidogenesis in the ovary and the expression of gonadotropin-related genes in the anterior pituitary was examined.

2. Materials and methods

2.1. Animals and treatments

C57BL/6J mice (CLEA Japan, Tokyo, Japan) were maintained on a 12-h light/12-h dark cycle (lights off at 2000 h) with controlled temperature (25 °C) and mice were given a commercial diet (MF, Oriental Yeast Co., Tokyo, Japan) and fresh tap water *ad libitum*. All animals were maintained in accordance with the NIH guide for the care and use of laboratory animals. All experiments were approved by the institutional animal care committee of the Yokohama City University. Female pups were given daily subcutaneous (s.c.) injections of 3 μg DES (Sigma Chemical Co., St. Luis, MO) dissolved in 0.02 ml sesame oil or the vehicle alone for 5 days starting on the day of birth. Female mice were killed by cervical dislocation and weighed at 1, 1.5, 2 or 3 months of age. Ovaries were weighed, fixed for histological analysis or frozen for quantitative real-time RT-PCR analysis.

Three-month-old C57 BL/6J mice treated neonatally with oil or DES were administered with 5 IU of PMSG intraperitoneally (i.p.) followed by 5 IU hCG 48 h later. Ovaries were dissected 8 h after the hCG injection and frozen for quantitative real-time RT-PCR.

αERKO mice were obtained by mating mice of a mixed C57BL6/129Sv background that were heterozygous for *Erα* disruption as described previously [34]. Female pups of wild-type (WT) and αERKO mice were given daily s.c. injections of 3 μg DES dissolved in sesame oil or vehicle alone for 5 days starting on the day of birth. Female mice were killed by cervical dislocation at 4 or 8 months of age. Ovaries were weighed and fixed for histological analysis.

2.2. Histological analysis

Left ovaries were fixed in Bouin's solution overnight, dehydrated through a graded series of ethanol, embedded in paraffin and serially sectioned at 8 μm. Sections were deparaffinized, hydrated through a graded series of ethanol and stained with hematoxylin and eosin (HE). Right ovaries were fixed in 10% formalin neutral buffer solution (Wako Pure Chemical Industries, Osaka, Japan) overnight, then immersed in 8% sucrose in phosphate buffered saline (PBS, pH 7.4). Frozen sections (6 μm thickness) were washed in purified water, rinsed with 60% isopropyl alcohol (Wako), stained with a freshly prepared Oil Red O (MERCK KGaA, Darmstadt, Germany) working solution at 37 °C for 15 min. Sections were rinsed with 60% isopropyl alcohol, washed in purified water and counterstained with hematoxylin. Four to 8 mice were examined in each group for histological analysis.

2.3. Immunohistochemistry

Left ovaries from oil- or DES-exposed mice were fixed in 4% paraformaldehyde (MERCK KGaA) in PBS at 4 °C overnight, embedded in paraffin and serially sectioned at 5 μm for CYP11A1, SF-1 and estrogen receptor β (ERβ) immunohistochemistry. Sections were mounted on silane (3-aminopropyl triethoxy-silane, Sigma)-coated glass slides, deparaffinized and hydrated through a graded series of ethanol. After washing in purified water, slides were microwaved for 5 min for SF-1 and 8 min for ERβ staining in 10 mM sodium citrate buffer (pH 6.0) for antigen retrieval. Endogenous peroxidase activity was blocked by 1% H_2O_2 in ion-exchanged water for 10 min. Then sections were washed in PBS and incubated with normal blocking serum (VECTASTAIN Elite ABC kit, Vecter Laboratories, Inc., Burlingame, CA) for CYP11A1 and ERβ staining and 5% bovine serum albumin (Sigma) in PBS for SF-1 staining for 30 min. After washing in PBS, sections were incubated with rabbit polyclonal antibody against rat CYP11A1 (1:5000 dilution, Chemicon International, Inc., Temecula, CA), rabbit polyclonal antibody against bovine SF-1 (1:10 000 dilution; a gift from Dr. Y. Ikeda, School of Mecidine, Yokohama City University), rabbit polyclonal antibody against mouse ERβ (1:250 dilution, Zymed Laboratories, San Francisco, CA), or rabbit immunoglobulin fraction (Dako Cytomation, Glostrup, Denmark) as a negative control at 4 °C overnight. For SF-1 and ERβ staining, sections were washed in PBS and incubated with biotinylated secondary antibody (Vector Laboratories) for 30 min. After washing in PBS, sections were incubated with avidin–biotin complex (ABC) reagents (Vector Laboratories) for 30 min according to the manufacturer's protocol. For CYP11A1 staining, sections were washed in PBS and incubated with histofine simple stain PO (R) (Nichirei Co., Tokyo, Japan) for 45 min. Reaction products were visualized using 1 mg/ml 3,3′-diaminobenzidine (DAB, Sigma) in PBS containing 1% H_2O_2 and sections were counterstained with hematoxylin. Five mice were examined in each group for immunohistochemical analysis.

2.4. Quantitative real-time RT-PCR

Ovaries from 1.5- and 3-month-old mice treated neonatally with oil or DES, and anterior pituitaries from 3-month-old mice treated neonatally with oil or DES were homogenized in TRIzol (Invitrogen Co., Carlsbad, CA). Total RNA isolated from ovaries and pituitaries was purified by DNase I (Roche, Penzberg, Germany) to remove genomic DNA, cleaned up with an RNeasy total RNA kit (Qiagen, Chatsworth, CA) and reverse transcribed into cDNA by SuperScript II reverse transcriptase (Invitrogen) using oligo dT primer (Invitrogen). Real-time PCR was carried out with a Smart Cycler II System (Takara Bio Inc., Otsu, Japan) with SYBR Premix Ex Taq™ (Takara). Relative mRNA expression of *Star*, *Cyp11a1*, *Cyp19*, *Hsd3b1*, *Hsd3b1*, *Hsd3b6*, *Hsd17b1*, *Hsd17b3*, *Sf-1*, *Lrh-1*, *Cga*, *Fshb*, *Lhb* and peptidylprolyl isomerase A (*Ppia*) was determined by the standard curve method. Primer sequences are indicated in Supplemental Table 1. *Ppia* was chosen as an internal standard to control for variability in amplification due to differences in starting mRNA concentration. One ovary or anterior pituitary per mouse was examined in each group and 3 (ovary) or 5 (pituitary) independent experiments were carried out for quantitative real-time RT-PCR analysis.

2.5. Radioimmunoassay

Neonatally oil- or DES-treated 1.5- and 3-month-old mice were anaesthetized with diethyl ether (Wako) and blood was collected via the ascending jugular vein into tubes. The serum was isolated by centrifugation at 3000 rpm for 15 min and stored at −80 °C before use. The serum E2 level was estimated by DPC ^{125}I radioimmunoassay kit, E2 double antibody, KE2D1 (Siemens Healthcare Diagnostics Inc., Los

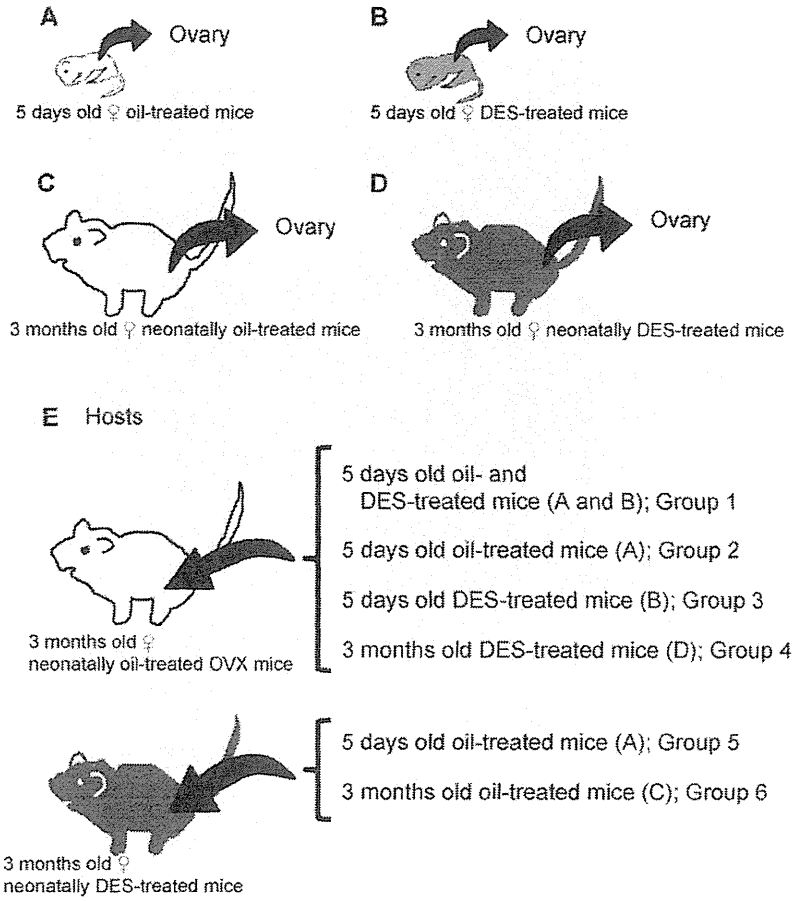

Fig. 1. Experimental design. White mice indicate neonatally oil-treated mice and black mice indicate neonatally DES-treated mice, respectively. Ovaries from 5-day-old oil- (A) or DES-treated mice (B) were transplanted under the renal capsule of the same ovariectomized adult mice (group 1), ovaries from 5-day-old oil-treated mice (A) were transplanted under the renal capsule of ovariectomized adult mice (group 2), ovaries from 5-day-old DES-treated mice (B) were transplanted under the renal capsule of ovariectomized adult mice (group 3), ovaries from 3-month-old mice treated neonatally with DES (D) were transplanted under the renal capsule ovariectomized adult mice (group 4), ovaries from 5-day-old oil-treated mice (A) were transplanted under the renal capsule of 3-month-old neonatally DES-treated adult mice (group 5), ovaries from 3-month-old oil-treated mice (C) were transplanted under the renal capsule of neonatally DES-treated 3-month-old mice (group 6), respectively. Ovx; ovariectomized mice.

Angeles, CA). The serum from each mouse was pooled up to 200 μl and 6–9 points were examined in each group for radioimmunoassay.

2.6. Tissue grafting

Six different groups of tissue grafting were shown in Fig. 1; ovaries from 5-day-old oil- or DES-treated mice were transplanted under the renal capsule of the same ovariectomized adult mice (group 1), ovaries from 5-day-old oil-treated mice were transplanted under the renal capsule of ovariectomized adult mice (group 2), ovaries from 5-day-old DES-treated mice were transplanted under the renal capsule of ovariectomized adult mice (group 3), ovaries from 3-month-old mice treated neonatally with DES were transplanted under the renal capsule ovariectomized adult mice (group 4), ovaries from 5-day-old oil-treated mice were transplanted under the renal capsule of neonatally DES-treated adult mice (group 5), and ovaries from 3-month-old oil-treated mice were transplanted under the renal capsule of neonatally DES-treated adult mice (group 6). At the end of the 3-month growth period, grafted ovaries were fixed in Bouin's solution or 10% formalin neutral buffer solution for histological analysis. Four to 9 host mice and 8–18 grafted ovaries were examined in each group for histological analysis.

2.7. Statistical analysis

Data are expressed as the mean ± standard error. For multiple comparisons, treatment groups were compared using analysis of variance (ANOVA) followed by Dunnett's post hoc test. Two-tailed Student's *t*-test was used for single comparison. Fisher's exact probability test was used to examine the significance of the association between the two kinds of classification. A statistically significant difference was defined as $p < 0.05$.

3. Results

3.1. Lipid accumulation in the ovary and involvement of ERα

Ovaries from 1-month-old neonatally oil- or DES-treated mice did not stain with Oil Red O (data not shown). CL in the ovaries of oil-treated mice were weakly stained with Oil Red O at 1.5 and 3 months of age (Fig. 2A and B). The interstitial and theca cells in the ovaries of neonatally DES-treated 1.5- and 3-month-old mice (Fig. 2A and B) stained with Oil Red O. In addition, the interstitial tissues of 3-month-old neonatally DES-treated mice showed medullary tubule-like structures. No CL was found in the ovary of 3-month-old neonatally DES-treated mice (Fig. 2A and B).

To examine the involvement of ERα in lipid accumulation, ovaries from 4- and 8-month-old neonatally oil- or DES-treated WT and αERKO mice were stained with Oil Red O. The interstitial tissue and CL in the ovaries of 4-month-old neonatally oil-treated WT mice slightly stained with Oil Red O (Fig. 2C). The interstitial regions of neonatally DES-treated WT mice showed medullary tubule-like structures. The interstitial and theca cells of neonatally DES-treated WT mice showed strong Oil Red O staining both in 4 and 8 months of age (Fig. 2D and H) and the stained area was increased in the ovaries of 8-month-old neonatally oil-treated WT mice (Fig. 2H). Ovaries from neonatally oil- or DES-treated αERKO mice showed

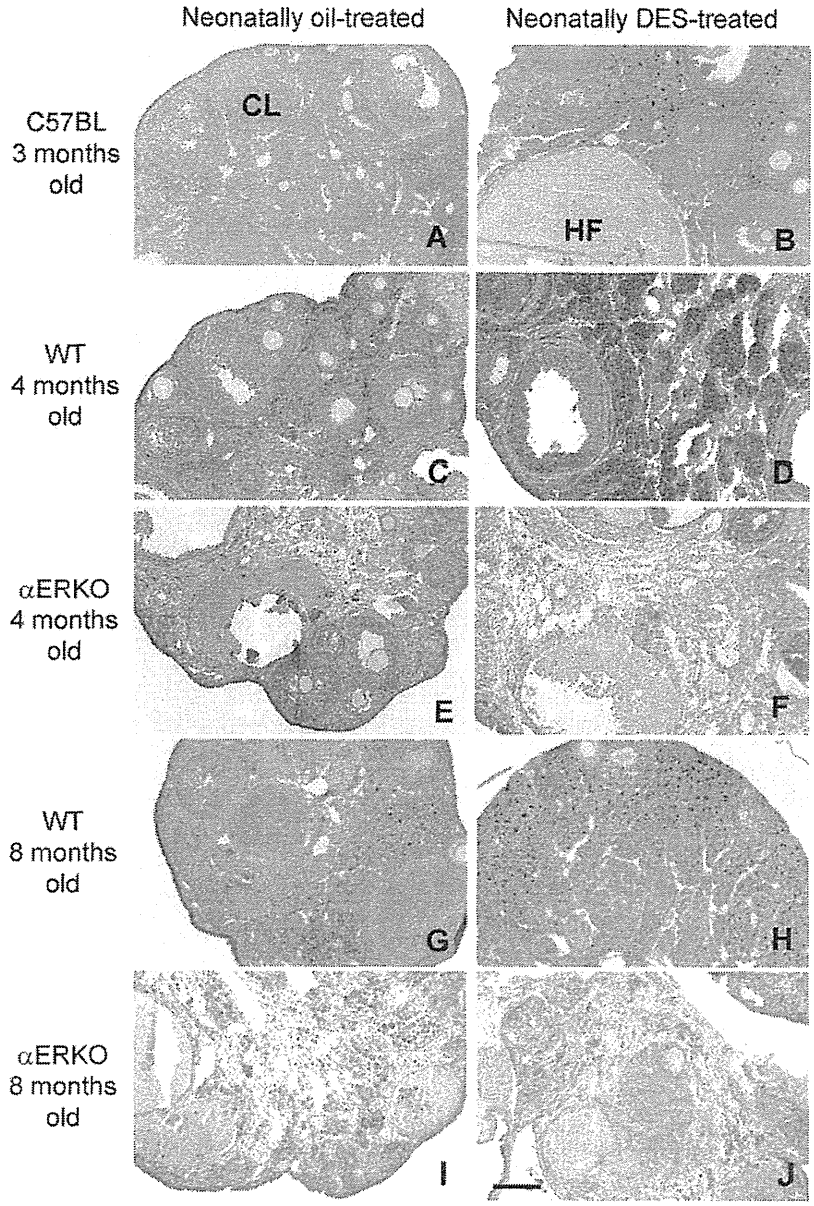

Fig. 2. Oil Red O staining in the ovary of neonatally oil- (A, C, E, G and I) or DES-treated (B, D, F, H and J) C56BL/6J (A and B), wild type (WT) (C, D, G and H) or ERα knockout (αERKO) mice (E, F, I and J), respectively. Ovaries from 3-month-old (A and B), 4-month-old (C–F) and 8-month-old (G–J) mice, respectively. CL; corpus luteum, HF; hemorrhagic follicle. Bar = 200 μm.

similar staining in the interstitial tissues with Oil Red O (Fig. 2E, F, I and J), but the stained area of the interstitial tissues was increased at 8 months of age both in the ovaries of neonatally oil- and DES treated αERKO mice (Fig. 2I and J).

3.2. Expression of genes involved in ovarian steroidogenesis

To examine the expression of genes involved in ovarian steroidogenesis in ovaries of oil- or DES-treated mice, real-time RT-PCR was performed. In 1.5-month-old neonatally DES-treated mice, the expression of *Star* was significantly decreased and the expression of *Lrh-1* was significantly increased compared with those in oil-treated mice (Fig. 3A). In 3-month-old neonatally DES-treated mice, the expression of *Star* and *Cyp11a1* was significantly decreased and the expression of *Cyp19* and *Sf-1* was significantly increased compared with those in oil-treated mice (Fig. 3A). The expression of *Hsd3b1*, *Hsd3b6*, *Hsd17b1* and *Hsd17b3* was not changed in neonatally DES-treated mice (Fig. 3B).

3.3. Localization of CYP11A1 and SF-1

CYP11A1 immunoreactivity localized in the cytoplasm of the interstitial and theca cells of both neonatally oil- and DES-treated mice at 1.5 and 3 months of age (Fig. 4A–D). The expression of CYP11A1 in the interstitial cells of 3-month-old neonatally DES-treated mice was slightly weaker than that in oil-treated mice (Fig. 4C and D). CL in the ovary of neonatally oil-treated 1.5- and 3-month-old mice also showed the expression of CYP11A1.

SF-1 immunoreactivity localized in the nuclei of the interstitial and theca cells of both 3-month-old oil- and DES-treated mice and the staining intensity was not changed in DES-treated mice (Fig. 4E and F).

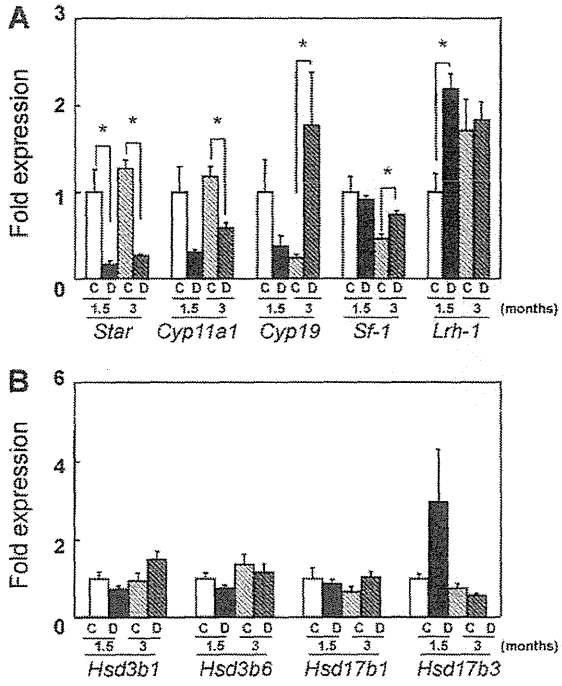

Fig. 3. Changes in the mRNA expression involved in ovarian steroidogenesis in the ovary of 1.5- and 3-month-old neonatally oil- or DES-treated C56BL/6J mice (A, B). C: neonatally oil-treated mice, D: neonatally DES-treated mice. *; $p < 0.05$, compared with age-matched oil-treated mice.

3.4. *Expression of Erα and Erβ mRNAs and ERβ protein*

The expression of *Erβ* mRNA in 1.5- and 3-month-old neonatally DES-treated mice was significantly increased compared with that in oil-treated mice, whereas *Erα* mRNA expression was not changed (Fig. 5B). The ERβ protein was found in the nuclei of granulosa cells both in oil- and DES-treated mice (Fig. 5C).

3.5. *Effects of gonadotropin treatments on the expression of genes involved in ovarian steroidogenesis*

Since genes involved in ovarian steroidogenesis are highly regulated by gonadotropins, and neonatally DES-treated mice showed reduced FSH levels [35], the effects of PMSG and hCG treatments on steroidogenesis in DES-treated mice were examined. The expression of *Star* was increased and *Cyp19*, *Sf-1* and *Erβ* expression was decreased by PMSG and hCG treatments both in 3-month-old neonatally oil- and DES-treated mice (Fig. 6A). The expression of *Cyp11a1* was increased only in 3-month-old neonatally DES-treated mice with PMSG and hCG treatments and there was similar expression in oil-treated mice.

3.6. *Serum 17β-estradiol levels and expression of gonadotropin-related genes in the anterior pituitary*

The serum E2 levels were not changed in neonatally DES-treated mice at 1.5 and 3 months of age compared with those in oil-treated mice (Fig. 6B). To examine the expression of genes involved in gonadotropins in pituitaries of oil- or DES-treated mice, real-time RT-PCR was performed. The expression of *Lhb* mRNA in 3-month-old neonatally DES-treated mice was

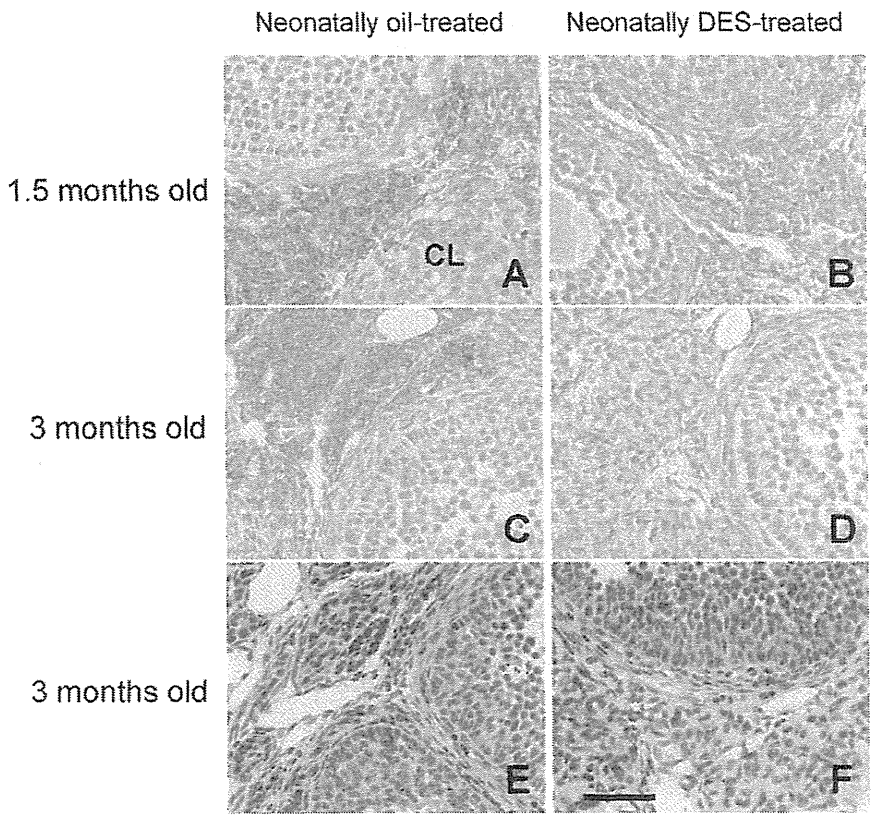

Fig. 4. Immunohistochemistry for CYP11A1 in the ovaries of 1.5-month-old neonatally oil-treated mice (A), 1.5-month-old neonatally DES-treated mice (B), 3-month-old neonatally oil control mice (C) and 3-month-old neonatally DES-treated mice (D). Immunohistochemistry for SF-1 in the ovary of 3-month-old neonatally oil-treated mice (E) and 3-month-old neonatally DES-treated mice (F). Bar = 50 μm. CL: corpus luteum.

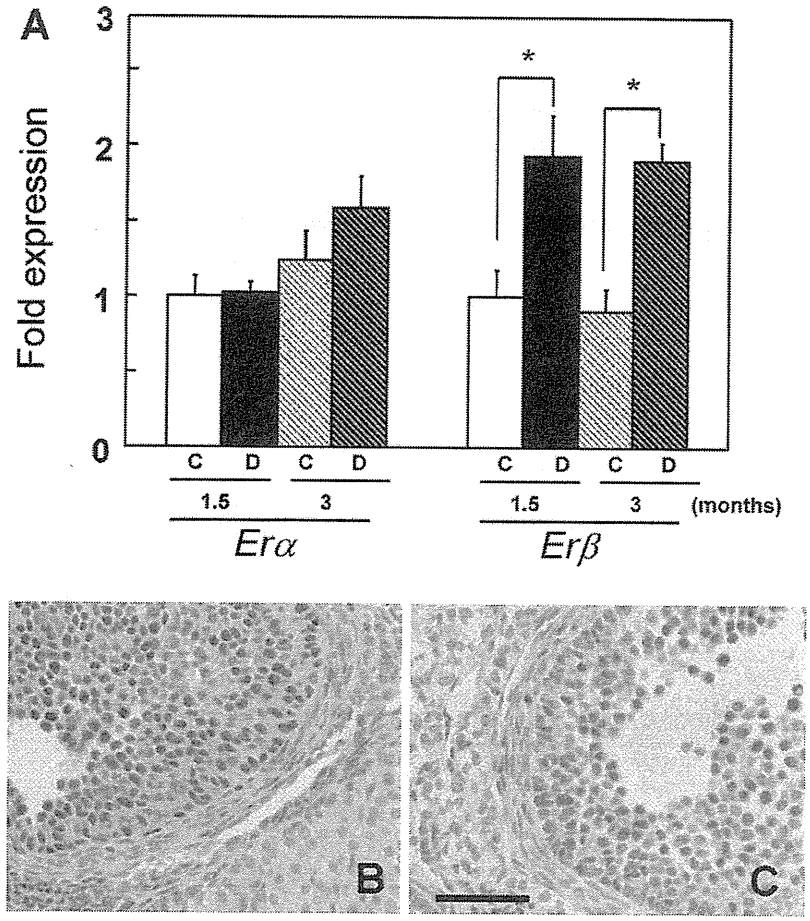

Fig. 5. mRNA expression in 1.5- and 3-month-old neonatally oil- or DES-treated C56BL/6J mice (A). C: neonatally oil-treated mice. D: neonatally DES-treated mice. Immunohistochemistry of ERβ in the 3-month-old neonatally oil- (B) and neonatally DES-treated mice (C). Bar = 50 μm. *; $p < 0.05$, compared with age-matched oil-treated mice.

significantly decreased compared with that in oil-treated mice, and *Cga* mRNA expression tended to be lower ($p = 0.068$, Fig. 6C). In contrast, *Fshb* mRNA expression was not changed (Fig. 6C). Ovariectomy stimulated the expression of *Cga*, *Fshb* and *Lhb* in the pituitary of 3-month-old neonatally oil-treated mice (data not shown).

3.7. Histology of grafted ovaries stained with Oil Red O

Various stages of follicles and CL (Fig. 7A and B) were found in both the grafted ovaries from neonatally oil- and DES-treated mice (group 1). Similarly, the grafted ovaries of neonatally oil- (group 2) and DES-treated mice (group 3) showed growing follicles and CL (Fig. 7C and D). Four out of 8 grafted ovaries in group 3 contained cystic follicles (CF) and 2 out of 8 grafted ovaries in group 3 contained hemorrhagic follicles (HF). Grafted ovaries of neonatally DES-treated 3-month-old mice (group 4) showed growing follicles, CL and CF (Fig. 7E). When ovaries of neonatally oil-treated 5-day-old (group 5) or 3-month-old mice were grafted into neonatally DES-treated mice (group 6), lipid droplets in interstitial and theca cells stained with Oil Red O were found and no CL was observed (Fig. 7F and G). The number of CL in ovaries of groups 2 and 3 were reduced compared to neonatally oil-treated 3-month-old mice (Table 1).

Table 1
Number of mice with corpora lutea (CL), cystic follicles (CF) and hemorrhagic follicles (HF) observed in neonatally oil- or DES-treated mice and grafted neonatally oil- or DES-treated ovaries.

Group	No. of mice examined	No. of mice with			Number of CLs in the ovary
		CL	CF	HF	
Oil-treated 3-month-old mice	7	7	0	0	6.4 ± 0.65
DES-treated 3-month-old mice	10	0[a]	4	3	0[a]
Oil-treated ovaries, group 1	7	5[b]	1	0	2.0 ± 0.65[a,b]
DES-treated ovaries, group 1	7	6[b]	5[a]	0	1.7 ± 0.42[a,b]
Oil-treated ovaries, group 2	7	6[b]	1	0	2.9 ± 0.69[a,b]
DES-treated ovaries, group 3	12	8[b]	4	2	1.9 ± 0.60[a,b]
DES-treated ovaries, group 4	4	4[b]	2	0	3.0 ± 0.58[a,b]

Number of CLs; the mean ± SE.
[a] $p < 0.05$; the significant difference from the oil-treated 3-month-old mice.
[b] $p < 0.05$; the significant difference from the DES-treated 3-month-old mice.

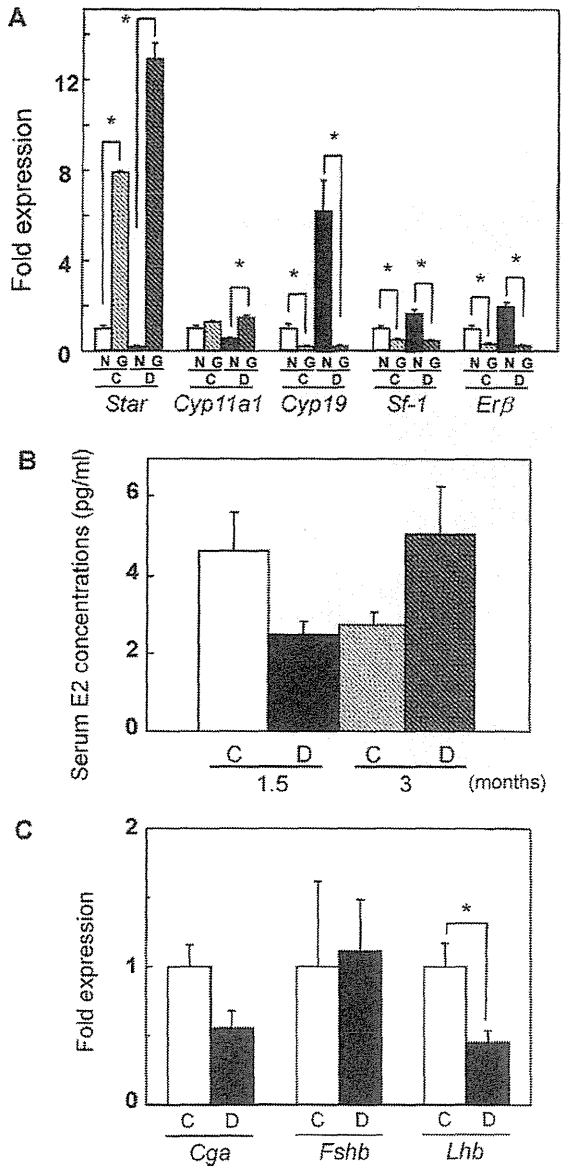

Fig. 6. Changes in the mRNA expression involved in ovarian steroidogenesis in the ovaries of 3-month-old neonatally oil- or DES-treated C56BL/6J mice after gonadotropin treatments (A) and serum levels of 17β-estradiol (E2) in 1.5- and 3-month-old neonatally oil- or DES-treated mice (B). Changes in the gonadotropin-related genes mRNA expression in the anterior pituitary of 3-month-old neonatally oil- or DES-treated C56BL/6J mice (C). N: non-treated with gonadotropins, G: treated with gonadotropins, C: neonatally oil-treated mice, D: neonatally DES-treated mice. *; $p < 0.05$ compared with age-matched oil control mice in the same treatment group.

Some grafted ovaries from groups 1, 3 and 4 had CF, and some grafted ovaries from group 3 also had HF (Table 1).

4. Discussion

Ovulation and steroidogenesis have begun by 1.5 months of age in neonatally oil-treated (Neo Oil) mice, since CL were observed in their ovaries. In contrast, CL were not found but lipid droplets were observed in the ovary of 1.5- and 3-month-old neonatally DES-treated (Neo-DES) mice, suggesting a lack of LH surge caused by neonatal DES treatment as previously reported [8].

The expression of *Star* and *Cyp11a1* was decreased in the ovary of 1.5- and 3-month-old Neo DES mice due to the alterations of gonadotropin levels [16,21,22]. Ronen-Fuhrmann et al. [36] showed that *Star* is expressed in interstitial and theca cells in response to PMSG, and then expressed in interstitial, theca and granulosa cells in response to hCG. *Cyp11a1* is also expressed in the interstitial, theca and granulosa cells in response to PMSG and reaches a peak after hCG administration. Thus, lack of the LH surge may result in a decrease of *Star* and *Cyp11a1* expression in Neo-DES mice. In addition, the expression of *Cyp19* increases in response to PMSG but decreases after hCG administration [36]. The expression of *Erβ* in the ovary is also reduced by hCG whereas PMSG has no effect [37]. In this study, the expression of *Star*, *Cyp11a1*, *Cyp19* and *Erβ* was restored after PMSG and hCG treatments in Neo-DES mice suggesting that insufficiency of gonadotropin levels. In addition, exogenous gonadotropins can affect steroidogenesis in the ovary of Neo-DES mice as well as oil-treated mice.

Hypertrophy of interstitial tissues is found in the ovaries of FSH receptor KO (FORKO) mice showing elevated levels of plasma FSH, LH and T, but decreased E2 levels with normal *Cyp19* expression compared with those in WT mice [38,39], and FSHβ subunit KO (FSHKO) mice showing decreased *Cyp11a1* and *Cyp19* despite high circulating levels of LH [19,40]. However, hypertrophy of interstitial tissues is not found in the ovary of αERKO mice showing high LH levels, normal FSH levels and *Star* and *Cyp11a1* expression [41]. Hasegawa et al. [12] showed that ovaries of *Star* KO mice appear normal, however, prominent lipid deposits accumulated in the interstitial region after the time of normal puberty. Targeted disruption of *Cyp11a1* results in the accumulation of lipid droplets in the interstitial cells [14]. Thus, hypertrophy and accumulation of lipid droplets in interstitial cells of Neo-DES mice is caused by failure of steroidogenesis due to the alterations of gonadotropin levels. Indeed, grafted ovaries of Neo-DES mice showed various stages of follicles and CL, but no lipid accumulation in the interstitial tissue, whereas grafted ovaries of Neo Oil mice into 3-month-old Neo-DES hosts showed lipid accumulation in the interstitial tissue. In addition, when ovaries from 1-month-old Neo-DES mice were grafted into control female hosts, the pattern of ^{3}H-steroids in *in vitro* steroid synthesis changes the pattern characteristic to controls and vice versa [4]. These results support the idea that hypertrophy of interstitial tissue in Neo-DES mice is caused by the alteration of gonadotropin levels and lack of the LH surge.

In Neo-DES mice, serum FSH concentrations are increased but LH levels are not altered on day 19 [35], however, the levels of FSH and LH are similar in Neo-Oil and Neo-DES mice on day 56 [42]. In males, the reduced concentrations of gonadotropins in plasma are observed in neonatally estrogenized rats [43]. In this study, the expression of *Lhb* was reduced but *Cga* and *Fshb* mRNA levels were not altered in the anterior pituitary of 3-month-old Neo-DES mice. In addition, the percentage of LH-producing cells in the anterior pituitary of Neo-DES mice was partially decreased at 3-month-old (unpublished data), suggesting that serum levels of gonadotropins may be altered in Neo-DES mice. Although the levels of FSH and LH in 3-month-old Neo-DES mice have not been investigated yet, it is speculated that reduced serum levels of gonadotropins in Neo-DES mice may result in hypertrophy of interstitial tissues in the ovary. Furthermore, the expression of gonadotropin-related genes is increased after ovariectomy [44] and our data were coincident with the previous reports, however, it is not clear whether ovariectomy can affect the pituitary gonadotropins in 3-month-old Neo-DES mice. Thus, it is necessary to examine the effects of neonatal DES treatment on the pituitary in the near future.

In this study, the serum levels of E2 were not different between Neo-Oil and Neo-DES mice although the expression of *Cyp19* was significantly increased in the ovary of Neo-DES mice. This fact suggests 2 possibilities: (1) transcription of *Cyp19* may be inhibited and/or (2) CYP19 may not have the ability to stimulate E2 synthesis in the ovary of Neo-DES mice. In addition, CYP19 is localized in

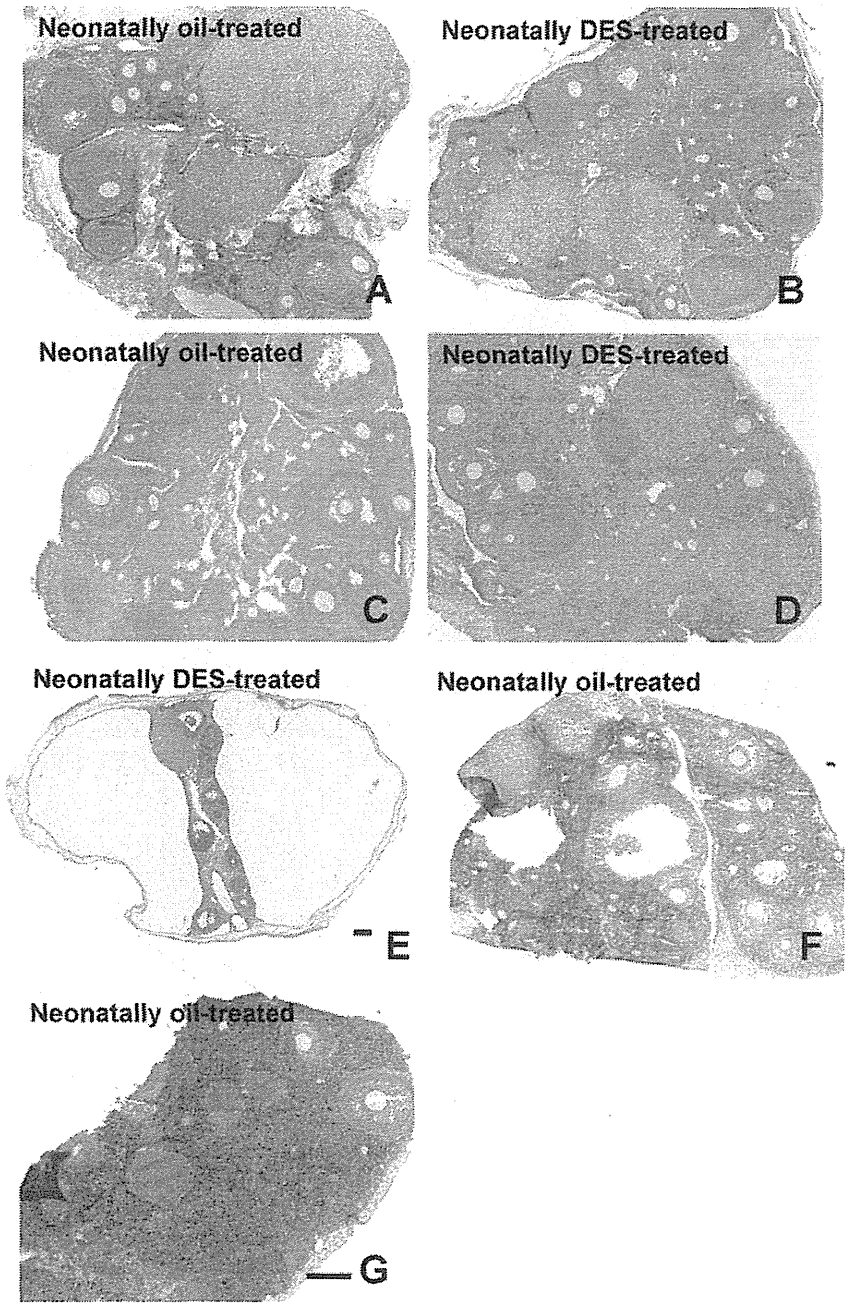

Fig. 7. HE and Oil Red O staining in grafted ovaries after the 3-month growth period. HE staining of the grafted ovaries from neonatally oil- (A) or DES-treated mice in 3-month-old neonatally oil-treated hosts (B, group 1). Oil Red O staining of the grafted ovaries from neonatally oil-treated mice (C, group 2), the grafted ovaries from neonatally DES-treated mice (D, group 3), the grafted ovaries from 3-month-old neonatally DES-treated mice (E, group 4) in 3-month-old neonatally oil-treated hosts, the grafted ovaries from neonatally oil-treated mice in 3-month-old neonatally DES-treated hosts (F, group 5) and the grafted ovaries from 3-month-old neonatally oil-treated mice in 3-month-old neonatally DES-treated hosts (G, group 6), respectively. Bar = 200 μm.

granulosa cells of the preovulatory follicle [15], therefore, it is possible that the function of granulosa cells can be altered in the ovary of Neo-DES mice. Indeed, inhibin secreted by granulosa cells is consisted of α and β subunits and the expression of inhibin α mRNA is high in the ovary of 2-month-old Neo-DES mice [45]. The number of oocytes is reduced in the Neo-DES mouse ovary [46,3]. Although the direct effects of neonatal DES treatments on oocytes are unclear, the oocyte–somatic cell interactions may also be impaired.

The expression of *Sf-1* is most abundant in the interstitial and theca cells in immature and cycling adult rats and also in granulosa cells of healthy growing follicles [33]. In this study, the expression of *Sf-1* both in the ovary of Neo-Oil or Neo-DES mice is significantly decreased with age, but *Sf-1* expression in the ovary of 3-month-old Neo-DES mice was higher than that in the age-matched Neo-Oil mice. Reduced expression of *Sf-1* after gonadotropin treatment is consistent with the previous report [33]. Thus, up-regulation of *Sf-1* in the ovary of 3-month-old Neo-DES mice may be due to lack of the LH surge. In contrast, the expression of *Lrh-1* is selective in granulosa and CL but not in interstitial and theca cells in cycling and immature rats [33]. Similar to *Sf-1*, the expression of *Lrh-1* in

the ovary is also decreased in response to the combination of E2, FSH and hCG treatments [33]. Interestingly, the expression of *Lrh-1* in the ovary of 1.5-month-old Neo-DES mice was significantly increased compared with that in the age-matched Neo-Oil mice, but not at 3 months of age. Both granulosa and luteal cells in the ovary of Neo-Oil mice may be responsible for the expression of *Lrh-1*, however, only granulosa cells may be involved in *Lrh-1* expression in the ovary of Neo-DES mice. In addition, *Sf-1* and *Lrh-1* have qualitatively similar actions on FSH-stimulated steroidogenesis in the ovary [24]. The localization of those genes raises the possibility that *Sf-1* may contribute to the interstitial and theca cells and *Lrh-1* may be specific for luteal cells, however, the function of these genes in granulosa cells where both genes are expressed is still unclear. Indeed, the expression of *Hsd3b1*, a target of both *Sf-1* and *Lrh-1* [15,47], was not altered in the ovary of Neo-DES mice. In the future study, therefore, it is needed to isolate different cell types from the ovaries of Neo-DES mice and quantify the expression of *Sf-1* and *Lrh-1*, respectively.

HSD17B1 is expressed in granulosa cells and converts estrone to E2, while HSD17B3 is expressed in Leydig cells and coverts androstenedione to T [15]. The ovary of αERKO mice exhibits testis-like levels of *Hsd17b3* expression [48]. The expression of *Hsd17b1* and *Hsd17b3* in the ovary of Neo-DES mice was not altered, suggesting that the interstitial and theca cells of Neo-DES mice maintain a female phenotype.

In this study, HF were occasionally found in the ovaries of Neo-DES mice, even after the grafting ovaries from Neo-DES mice into the normal host mice. HF are also seen in the ovaries of αERKO mice due to the high circulating levels of LH [49] but not in βERKO mice [50]. The transgenic LHβ-C-terminal peptide (LHβCTP) mice exhibiting LH hypersecretion also show HF, however, LHβCTP mice lacking ERβ show no HF [51]. In addition, in αERKO mice, plasma levels of FSH, and expression of *Star* and *Cyp11a1* expression are normal but the expression of *Cyp17* and *Cyp19* is elevated in the ovary [41]. Therefore, HF in the ovary of Neo-DES mice is not due to high circulating levels of LH and elevated steroidogenesis as in αERKO. Previously, we reported that neonatal DES treatment inhibited follicle formation and development through ERβ in the neonatal mouse ovaries [52], indicating that DES may directly affect follicular growth and development.

In summary, our findings indicate that hypertrophy and accumulation of lipid droplets in ovarian interstitial cells of Neo-DES mice is caused by impaired steroidogenesis due to low levels of gonadotropins, especially lack of the LH surge. Neonatal DES treatment can affect the HPG axis via ERα and indirectly disrupt ovarian steroidogenesis.

Conflict of interest statement

There is no conflict of interest.

Acknowledgements

We thank Dr. Yayoi Ikeda, Yokohama City University School of Medicine, for supplying the rabbit polyclonal antibody against bovine SF-1, and Dr. Raphael Guzman, Department of Molecular Cell Biology and Cancer Research Laboratory of University of California at Berkeley, for his critical reading of this manuscript.

Appendix A. Supplementary data

Supplementary data associated with this article can be found, in the online version, at doi:10.1016/j.reprotox.2011.10.013.

References

[1] Herbst AL. Clear cell adenocarcinoma and the current status of DES-exposed females. Cancer 1981;48:484–8.
[2] Takasugi N, Bern HA, DeOme KB. Persistent vaginal cornification in mice. Science 1962;137:138–9.
[3] Haney AF, Newbold RR, McLachlan JA. Prenatal diethylstilbestrol exposure in the mouse: effects on ovarian histology and steroidogenesis in vitro. Biol Reprod 1984;30:471–8.
[4] Tenenbaum A, Forsberg JG. Structural and functional changes in ovaries from adult mice treated with diethylstilboestrol in neonatal period. J Reprod Fertil 1985;73:465–77.
[5] Iguchi T, Takasugi N. Polyovular follicles in the ovary of immature mice exposed prenatally to diethylstilbestrol. Anat Embryol 1986;175:53–5.
[6] Iguchi T. Cellular effecs of early exposure to sex hormones and antihormones. Int Rev Cell Mol Biol 1992;139:1–57.
[7] Couse JF, Dixon D, Yates M, Moore AB, Ma L, Maas R, et al. Estrogen receptor-alpha knockout mice exhibit resistance to the developmental effects of neonatal diethylstilbestrol exposure on the female reproductive tract. Dev Biol 2001;538:224–38.
[8] Aihara M, Hayashi S. Induction of persistent diestrus followed by persistent estrus is indicative of delayed maturation of tonic gonadotropin-releasing systems in rats. Biol Reprod 1989;40:96–101.
[9] Hayashi S, Aihara M, Wakabayashi K. Content and distribution pattern of luteinizing hormone-releasing hormone (LHRH) in the hypothalamus of neonatally estrogenized female rats. Neurosci Res 1991;12:366–78.
[10] Döhler KD, Jarzab B, Sickmöller PM, Kokociñska D, Kaminski M, Gubala E, et al. Influence of neurotransmitters on sexual differentiation of brain structure and function. Exp Clin Endocrinol 1992;98:99–109.
[11] Halling A, Forsberg JG. Plasma testosterone levels and ovarian testosterone content in adult mice treated with diethylstilbestrol neonatally. J Steroid Biochem 1989;32:439–43.
[12] Hasegawa T, Caron LZKM, Majdic G, Suzuki T, Shizawa S, Sasano H, et al. Developmental roles of the steroidogenic acute regulatory protein (StAR) as revealed by StAR knockout mice. Mol Endocrinol 2000;14:1462–71.
[13] Ishii T, Hasegawa T, Pai C, Yvgi-Ohana N, Timberg R, Zhao L, et al. The roles of circulation high-density lipoproteins and trophic hormones in the phenotype of knockout mice lucking the steroidogenic acute regulatory protein. Mol Endocrinol 2002;16:2297–309.
[14] Hu M-C, Hsu N-C, Hadj NBE, Pai C-I, Chu H-P, Wang C-KL, et al. Steroid deficiency syndromes in mice with targeted disruption of Cyp11a1. Mol Endocrinol 2002;16:1943–50.
[15] Payne AH, Hales DB. Overview of steroidogenic enzymes in the pathway from cholesterol to active steroid hormones. Endocr Rev 2004;25:947–70.
[16] Lavoie HA, King SR. Transcriptional regulation of steroidogenic genes: STARD1, CYP11A1 and HSD3B. Exp Biol Med 2009;234:880–907.
[17] Craig J, Orisaka M, Wang H, Orikasa S, Thompson W, Zhu C, et al. Gonadotropin and intra-ovarian signals regulating follicle development and atresia: the delicate balance between life and death. Front Biosci 2007;12:3628–39.
[18] Fizpatrick SL, Richards JS. Regulation of cytochrome P450 aromatase messenger riobonucleic acid and activity by steroids and gonadotropins in rat granulosa cells. Endocrinology 1991;129:1452–62.
[19] Burns KH, Yan C, Kumar TR, Matzuk MM. Analysis of ovarian gene expression in follicle-stimulating hormone β knockout mice. Endocrinology 2001;142:2742–51.
[20] Fizpatrick SL, Carlone DL, Robker RL, Richards JS. Expression of aromatase in the ovary: down-regulation of mRNA by the ovulatory luteinizing hormone surge. Steroids 1997;62:197–206.
[21] Oonk RB, Krasnow JS, Beattie WG, Richards JS. Cyclic AMP-dependent and -independent regulation of cholesterol side chain cleavage cytochrome P-450 (P-450scc) in rat ovarian granulosa cells and corpora lutea. cDNA and deduced amino acid sequence of rat P-450scc. J Biol Chem 1989;264:21934–42.
[22] Stocco C, Telleria C, Gibori G. The molecular control of corpus luteum formation, function, and regression. Endocr Rev 2007;28:117–49.
[23] Hinshelwood MM, Repa JJ, Shelton JM, Richardson JA, Mangelsdorf DJ, Mendelson CR. Expression of LRH-1 and SF-1 in the mouse ovary: localization in different cell types cprrelates with differing function. Mol Cell Endocrinol 2003;207:39–45.
[24] Saxena D, Escamilla-Hernandez R, Little-Ihring L, Zeleznik AJ. Liver receptor homolog-1 and steroidogenic factor-1 have similar actions on rat granulosa cell steroidogenesis. Endocrinology 2007;148:726–34.
[25] Ikeda Y, Lala DD, Luo X, Kim E, Moisan MP, Parker KL. Characterization of the mouse FTZ-F1 gene, which encodes a key regulator of steroid hydroxylase gene expression. Mol Endocrinol 1993;7:852–60.
[26] Morohashi K, Iida H, Nomura M, Hatano O, Honda S, Tsukiyama T, et al. Functional difference between Ad4BP and ELP, and their distributions in steroidogenic tissues. Mol Endocrinol 1994;8:643–53.
[27] Sugawara T, Holt JA, Kiriakidou M. Strauss JF3rd. Steroidogenic factor 1-dependent promoter activity of the human steroidogenic acute regulatory protein (StAR) gene. Biochemistry 1996;35:9052–9.
[28] Morohashi K, Honda S, Inomata Y, Handa H, Omura T. A common *trans*-acting factor, Ad4-binding protein, to the promoters of steroidogenic P-450s. J Biol Chem 1992;267:17913–9.

[29] Carlone DL, Richards JS. Functional interactions, phosphorylation, and levels of 3′,5′-cyclic adenosine monophosphate-regulatory element binding protein and steroidogenic factor-1 mediate hormone-regulated and constitutive expression of aromatase in gonadal cells. Mol Endocrinol 1997;11:292–304.
[30] Jeyasuria P, Ikeda Y, Jamin SP, Zhao L, De Rooij DG, Themmen AP, et al. Cell-specific knockout of steroidogenic factor 1 reveals its essential roles in gonadal function. Mol Endocrinol 2004;18:1610–9.
[31] Duggavathi R, Volle DH, Mataki C, Antal MC, Messaddeq N, Auwerx J, et al. Liver receptor homolog 1 is essential for ovulation. Genes Dev 2008;22:1871–6.
[32] Zhao H, Li Z, Cooney AJ, Lan ZJ. Orphan nuclear receptor function in the ovary. Front Biosci 2007;12:3398–405.
[33] Falender AE, Lanz R, Malenfant D, Belanger L, Richards JS. Differential expression of steroidogenic factor-1 and FTF/LRH-1 in the rodent ovary. Endocrinology 2003;144:3598–610.
[34] Dupont S, Kust A, Gansmuller A, Dierich A, Chambon P, Mark M. Effect of single and compound knockouts of estrogen receptor α (ERα) and β (ERβ) on mouse reproductive phenotypes. Development 2000;127:4277–91.
[35] Kipp JL, Kilen SM, Bristol-Gould S, Woodruff TK, Mayo KE. Neonatal exposure to estrogens suppresses activin expression and signaling in the mouse ovary. Endocrinology 2007;148:1968–76.
[36] Ronen-Fuhrmann T, Timberg R, King SR, Hales KH, Hales DB, Stocco DM, et al. Spatio-temporal expression patterns of steroidogenic acute regulatory protein (StAR) during follicular development in the rat ovary. Endocrinology 1998;139:303–15.
[37] Couse JF, Bunch DO, Lindzey J, Schomberg DW, Korach KS. Prevenion of the polycystic ovarian phenotype and characterization of ovulatory capacity in the estrogen receptor-α knockout mouse. Endocrinology 1999;140: 5855–65.
[38] Danilovich N, Babu PS, Xing W, Gerdes M, Krishnamurthy H, Sairam MR. Estrogen deficiency, obesity, and skeletal abnormalities in follicle-stimulating hormone receptor knockout (FORKO) female mice. Endocrinology 2000;141:4295–308.
[39] Danilovich N, Roy I, Sairam MR. Ovarian pathology and high incidence of sex cord tumors in follitropin receptor knockout (FORKO) mice. Endocrinology 2001;142:3673–84.
[40] Abel MH, Huhtaniemi I, Pakarinen P, Kumar TR, Charlton HM. Age-related uterine and ovarian hypertrophy in FSH receptor knockout and FSHβ subunit knockout mice. Reproduction 2003;125:165–73.
[41] Couse JF, Yates MM, Walker VR, Korach KS. Characterization of the hypothalamic–pituitary–gonadal axis in estrogen receptor (ER) null mice reveals hypergonadism and endocrine sex reversal in females lacking ERalpha but not ERbeta. Mol Endocinol 2003;17:1039–53.
[42] Halling A. Alterations in hypothalamic and pituitary hormone levels induced by neonatal treatment of female mice with diethylstilbestrol. Reprod Tox 1992;16:335–46.
[43] Aguilar R, Bellido C, Benitez de Lupo EA. Differences in prepuberal neonatally estrogenized or androgenized male rats. Andrologia 1987;19:183–7.
[44] Gharib SD, Wierman ME, Shupnik MA, Chin WW. Molecular biology of the pituitary gonadotropins. Endocrine Rev 1990;11:177–99.
[45] Kirigaya A, Kim H, Hayashi S, Chambon P, Watanabe H, Iguchi T, et al. Involvement of estrogen receptor β in the induction of polyovular follicles in mouse ovaries exposed neonatally to diethylstilbestrol. Zool Sci 2009;26:704–12.
[46] McLachlan JA, Newbold RR, Shah HC, Hogan MD, Dixon RL. Reduced fertility in female mice exposed transplacentally to diethylstilbestrol (DES). Fertil Steril 1982;38:364–71.
[47] Peng N, Kim JW, Rainey WE, Carr BR, Attia CR. The role of the orphan nuclear receptor, liver receptor homologue-1, in the regulation of human corpus luteum 3beta-hydroxysteroid dehydrogenase type II. J Clin Endocrinol Metabol 2003;88:6020–8.
[48] Couse JF, Yates MM, Rodriguez KF, Johnson JA, Poirier D, Korach KS. The intraovarian actions of estrogen receptor-alpha are necessary to repress the formation of morphological and functional Leydig-like cells in the female gonad. Endocrinology 2006;147:3666–78.
[49] Schomberg DW, Couse JF, Mukherjee A, Lubahn DB, Sar M, Mayo KE, et al. Targeted disruption of the estrogen receptor-a gene in female mice: characterization of ovarian responses and phenotype in the adult. Endocrinology 1999;140:2733–44.
[50] Krege JH, Hodgin JB, Couse JF, Enmark E, Warner M, Mahler JF, et al. Generation and reproductive phenotypes of mice lacking estrogen receptor beta. Proc Natl Acad Sci USA 1998;95:15677–82.
[51] Couse JF, Yates MM, Sanford R, Nyska A, Nilson JH, Korach KS. Formation of cystic ovarian follicles associated with elevated luteinizing hormone requires estrogen receptor-β. Endocrinology 2004;145:4693–702.
[52] Kim H, Nakajima T, Hayashi S, Chambon P, Watanabe H, Iguchi T, et al. Effects of diethylstilbestrol on programmed oocyte death and induction of polyovular follicles in neonatal mouse ovaries. Biol Reprod 2009;81:1002–9.

ZOOLOGICAL SCIENCE 29: 377–383 (2012)

Transforming Growth Factor-α mRNA Expression and Its Possible Roles in Mouse Endometrial Stromal Cells

Tetsuya Maekawa[1], Atsuko Sakuma[1], Shusuke Taniuchi[1], Yuki Ogo[1], Taisen Iguchi[2], Sakae Takeuchi[1], and Sumio Takahashi[1]*

[1]*Department of Biology, The Graduate School of Science and Technology, Okayama University, Tsushima, Kita-ku, Okayama 700-8530, Japan*
[2]*Division of Molecular Environmental Endocrinology, Department of Environmental Biology, National Institute for Basic Biology, Okazaki, Aichi 444-8585, Japan*

Transforming growth factor-α (TGFα) is thought to be involved in the regulation of endometrial cells. We investigated *Tgfa* mRNA expression, and the effects of TGFα on DNA-synthesis and gene expression of insulin-like growth factor 1 (IGF1), IGF binding protein-3 (IGFBP3) and IGF1 receptor in the mouse endometrial cells, because IGF1 is involved in estrogen-induced growth of endometrial cells. We also investigated the role of TGFα on matrix metalloproteinase (MMP) expression, as MMPs are involved both in tissue remodeling during cell proliferation and in enhancement of IGF1 signaling through the degradation of IGFBP3. *Tgfa* mRNA expression was detected in endometrial luminal and glandular epithelial cells, and stromal cells. *Tgfa* mRNA signals did not appear to change in endometrial luminal epithelial cells, but signals in glandular epithelial cells were higher at diestrus 1, 2 and proestrus, and the number of stromal cells showing strong signals appeared to increase at diestrus 1 and 2. Endometrial epithelial and stromal cells were treated with estradiol-17β (E2) or progesterone (P4). E2 or P4 stimulated *Tgfa* mRNA expression in stromal cells. TGFα stimulated DNA synthesis in endometrial epithelial and stromal cells, while E2 and P4 stimulated DNA synthesis in stromal cells. In stromal cells, TGFα, at as low as 1 ng/ml, decreased *Igfbp3* and *Mmp9* mRNA levels, while high dose (10 ng/ml) of TGFα decreased *Igf1* mRNA level and increased *Mmp3* mRNA level. These results imply that TGFα stimulates proliferation of endometrial stromal cells through multiple mechanisms, including its regulation of *Igfbp3* and *Mmp3* transcription.

Key words: TGFα, endometrium, uterus, mouse, reproduction

INTRODUCTION

The mammalian endometrium consists of a single layer of epithelial cells and underlying stromal cells. Ovarian steroid hormones, estrogen and progestin, are involved in the proliferation of endometrial cells. Estrogen stimulates the proliferation of endometrial epithelial cells, while simultaneous treatment with estrogen and progestin stimulates the proliferation of endometrial stromal cells in adult mice (Huet-Hudson et al., 1989). A similar combined action of estrogen and progestin occurs at peri-implantation period. The proliferative effects of steroid hormones are mediated by various growth factors, including epidermal growth factor (EGF), insulin-like growth factor-1 (IGF1), and basic fibroblast growth factor (bFGF) (Tomooka et al., 1986; DiAugustine et al., 1988; Beck and Garner, 1992; Das et al., 1994; Cooke et al., 1997; Sato et al., 2002; Inoue et al., 2005). Besides growth factors, extracellular matrix (ECM) plays an important role in the regulation of cell proliferation and functions (Giancotti and Ruoslahti, 1999; Hotary et al., 2003). Hence, synthesis and breakdown of ECM components need to be studied for understanding of regulatory mechanisms of endometrial cells.

Transforming growth factor-α (TGFα), which comprises 50 amino acids, is a member of the EGF family and binds to epidermal growth factor receptor (EGFR), and is a mitogenic factor for various cell types, such as breast cancer cells, prostate epithelial cells and pituitary cells (Reddy et al., 1994; Itoh et al., 1998; Sharma et al., 2003). The stimulatory role of TGFα on the progression of decidualization has been reported in humans and rats (Taga et al., 1997; Tamada et al., 2001). TGFα is also a candidate growth factor involved in the regulation of endometrial cell proliferation, as TGFα and EGFR are both expressed in the mouse uterus (Tamada et al., 1991). Moreover, treatment with a specific antibody for rat TGFα suppressed estrogen-induced endometrial epithelial cell proliferation in vivo (Nelson et al., 1992). In addition, our previous study revealed that estradiol-17β (E2) plus progesterone (P4), in addition to TGFα, stimulated the proliferation of endometrial stromal cells (Komatsu et al., 2003). These findings suggest that TGFα is involved in the regulation of cell proliferation in the mouse uterus. However, the effects of estrogen and progestin on *Tgfa* mRNA expression in each mouse endometrial cell are unclear. Therefore, in the present study, we investigated

* Corresponding author. Tel. : +81-86-251-7866;
Fax : +81-86-251-7876;
E-mail: stakaha@cc.okayama-u.ac.jp
doi:10.2108/zsj.29.377

Tgfa mRNA expression in the mouse endometrium by in situ hybridization, and changes in *Tgfa* mRNA expression in response to E2 and/or P4 in cultured endometrial cells. We also investigated the effects of TGFα on DNA-synthesis and gene expression of the IGF system including IGF1, IGF binding protein-3 (IGFBP3) and IGF1 receptor (IGF1R), because IGF1 is one of the main growth factors involved in estrogen-induced growth of endometrial cells (Zhu and Pollard, 2007).

ECM components, including collagen types I, III, and IV, fibronectin and laminin have been detected in the endometrium (Aplin et al., 1988; Iwahashi et al., 1997; Nuttall and Kennedy, 2000a). Degradation of ECM components in endometrial tissues is associated with proliferation and mobility change of endometrial cells (Curry and Osteen, 2003; Russo et al., 2009), and is regulated by matrix metalloproteinases (MMPs), a family of ECM degrading enzymes. The MMP family is divided into several distinct subgroups: collagenases, gelatinases, stromelysins, and membrane type MMPs (Curry and Osteen, 2003). Collagenases are enzymes that degrade fibrillar collagen. Gelatinases (MMP2 and MMP9) degrade denatured collagen and major components of the basement membrane. Stromelysins (MMP3) act on a broad range of ECM components, including different types of collagens, fibronectin, laminin and vitronectin. MMPs may be involved in ovarian steroid hormone-induced remodeling of endometrial tissues. We therefore also investigated the involvement of TGFα on MMP2, MMP3 and MMP9 expression in endometrial cells.

MATERIALS AND METHODS

Animals

Immature (21–23 days old) and adult (eight weeks old) female mice of the ICR strain were used. They were housed in a temperature-controlled animal room, and were fed a commercial diet (CA-1; CLEA Japan Inc., Osaka, Japan) and tap water. Vaginal smear sampling was conducted daily in the morning for at least two weeks. Animal care and all experiments were performed in accordance with the Guidelines for Animal Experimentation of Okayama University, Japan.

Real-time PCR

Total RNA was prepared from cultured endometrial cells using a single-step method (Chomczynski and Sacchi, 1987). Total RNA was reverse-transcribed using Thermoscript Reverse Transcriptase (Invitrogen, CA, USA) according to the manufacturer's instructions. Oligo(dT) primers were used for the RT reactions.

Primer sets for real-time RT-PCR reactions were designed and are summarized in Table 1. Real-time PCR analysis was conducted using Applied Biosystems 7300 Real-Time PCR System (Foster City, CA, USA) and SYBR Premix Ex Taq (Takara Bio, Otsu, Japan). Amplifications were done in 15-μl aliquots according to the manufacturer's instructions. DNA polymerase was activated by heating at 95°C for 10 sec, followed by 40 cycles of amplification including denaturation at 95°C for 5 sec and annealing at 60°C for 31 sec. The expression of each mRNA was normalized to the expression of ribosomal protein L19 (*Rpl19*) mRNA.

Riboprobes

A DNA fragment encoding part of the mouse *Tgfa* (310–755) was obtained by RT-PCR. The cDNA fragment was subcloned into a pGEM-3zf(+) vector at the *EcoRI* and *HindIII* sites. One clone was sequenced using fluorescein primers (BigDye Terminator v3.1 Cycle Sequencing Kit, Applied Biosystems, Foster City, CA, USA) and an automated DNA sequencer (ABI PRISM™ 310 Genetic Analyzer, Applied Biosystems), and was confirmed to represent the cDNA encoding part of the mouse *Tgfa*. The plasmid DNA was linearized using restriction enzymes and RNA probes were synthesized using a T7 and SP6 polymerase system (Promega, Madison, WI, USA) according to the manufacturer's instructions. The probes were labeled with biotin-16-UTP (Roche Diagnostics, Mannheim, Germany).

Table 1. Primer sequence used for real-time PCR.

Name	Sequence	Length (bp)
Tgfa		
Forward	ATCCTGTTAGCTGTGTGCCA	105
Reverse	GGAATCTGGGCACTTGTTGA	
Egfr		
Forward	GCATCCGCAAGTGTAAAAAATGT	64
Reverse	CCAATGCCTATGCCATTACAAA	
Igf1		
Forward	AAAGCAGCCCGCTCTATCC	57
Reverse	CTTCTGAGTCTTGGGCATGTCA	
Igf1r		
Forward	GCTTCTGTGAACCCCGAGTATTT	82
Reverse	TGGTGATCTTCTCTCGAGCTACCT	
Igfbp3		
Forward	AAGCACCTACCTCCCCTCCCAA	98
Reverse	TGCTGGGGACAACCTGGCTTTC	
Mmp2		
Forward	GATGCTGCCTTTAACTGGAG	96
Reverse	CGGGTCCATTTTCTTCTTCACTTC	
Mmp3		
Forward	ACTTTCCAGGTGTTGACTC	80
Reverse	CTGCGAAGATCCACTGAAGAA	
Mmp9		
Forward	CTGGTGTGCCCTGGAACTCA	90
Reverse	GGAAACTCACACGCCAGAAGAA	
Rpl19		
Forward	CCCGTCAGCAGATCAGGAA	58
Reverse	GTCACAGGCTTGCGGATGA	

In situ hybridization

Localization of *Tgfa* mRNA in uterine tissue sections was determined by in situ hybridization, as previously described (Weiser et al., 1993). Uteri obtained from female mice of various ages were immediately fixed with 4% paraformaldehyde in 0.01 M phosphate-buffered saline (PBS) at room temperature overnight. They were processed for paraffin embedding and sectioned at 5-μm thickness. The sections were digested with 10 mg/ml proteinase K (Nacalai Tesque, Kyoto, Japan) at 37°C for 30 min and the proteinase K reaction was stopped with 0.2% (w/v) glycine in 0.01 M PBS. Sections were post-fixed with 4% paraformaldehyde in 0.01 M PBS, followed by acetylation treatment with 0.1 M triethanolamine (pH 8.0) and dehydrated. The uterine sections were placed in a moist chamber and hybridized at 50°C overnight in a solution containing 2× SSC, 1× Denhardt's solution, 10% dextran sulfate, 10 mM DTT, 2 mg yeast rRNA, 50% (v/v) deionized formamide and biotin-labeled sense or antisense *Tgfa* riboprobes. The slides were washed twice for 5 min in 1× SSC at room temperature, then twice for 10 min in 0.2× SSC at 50°C. Unhybridized RNAs and nonspecific signals were digested using RNase A (100 mg/ml) at 37°C for 30 min, after this slide were washed in 0.2× SSC at 50°C for 30 min, and dehydrated. Hybridization signals were visualized using Vectastain ABC kit (Vector, Burlingame, CA, USA)

Cell isolation

The isolation of uterine epithelial and stromal cells was performed as previously described (Ross et al., 1993; Shiraga et al., 1997; Komatsu et al., 2003). The isolated endometrial epithelial

cells were seeded on collagen-coated culture wells at a density of about 5×10^4 cells/cm^2. The isolated stromal cells separated from epithelial cells were seeded on poly-L-lysine coated culture wells at a density of about 6×10^4 cells/cm^2. First, the stromal cells were cultured in a 1:1 mixture of Dulbecco's modified Eagle's medium and Ham's F-12 medium without phenol red (DME/F12, Sigma Aldrich, St. Louis, MO, USA) containing 2% dextran-coated charcoal-treated fetal bovine serum. After pre-culture for 1-day, the cells were cultured in serum-free DME/F12 supplemented with BSA (1 g/l), hydrocortisone (100 μg/l), triiodothyronine (400 ng/l), transferrin (10 mg/l), glucagon (10 ng/l), parathormone (200 ng/l), sodium selenite (5 μg/l), and insulin (100 μg/l). The plates were incubated at 37°C in an atmosphere of 5% CO_2, and the medium was changed every two days.

Estradiol-17β (E2, Sigma Aldrich) and progesterone (P4, Sigma Aldrich) were initially dissolved in ethanol and at a stock concentration of 10 μM (0.03% and 0.01% ethanol, respectively). Working solutions of E2 and P4 were made by diluting the stock solution with culture media.

Determination of cell proliferation

The number of DNA synthesizing cells was investigated by 5'-bromo-2'-deoxyuridine (BrdU) incorporation using Cell Proliferation ELISA, BrdU kit (Roche Diagnostics). Cultured cells were treated with E2, P4, recombinant human TGFα (R&D systems, Minneapolis, MN, USA), or polyclonal goat anti-human TGFα antibody (R&D systems, cat. no. AB-239-NA) for 24 hr. The cells were exposed to 100 μM BrdU for the last 2 hr of incubation. Then, the cells were fixed and incubated with anti-BrdU monoclonal antibody from mouse–mouse hybrid cells conjugated with peroxidase (Anti-BrdU-POD). After washing, tetramethyl-benzidine was added as a substrate. This substrate reaction was stopped by the addition of 0.2 M sulfuric acid and the absorbance was measured at 450 nm.

Statistical analysis

The data are presented as the means ± SEM. Statistical analysis was carried out using analysis of variance followed by Tukey HSD test. Steel-Dwass method was used for comparison of populations that were not normally distributed.

RESULTS

Expression of *Tgfa* mRNA in the uteri of adult female mice during the estrous cycle

Tgfa mRNA levels in the whole uterus were analyzed at 24-hr intervals during the estrous cycle, and did not change during the estrous cycle (Fig. 1). *Egfr* mRNA levels were also analyzed and did not change during the estrous cycle (Fig. 1). The expression of *Tgfa* mRNA in the uteri of adult female mice during the estrous cycle was examined by in situ hybridization analysis using a *Tgfa* antisense riboprobe. The *Tgfa* sense riboprobe was used as a negative control for in situ hybridization. *Tgfa* mRNA signals were detected in endometrial luminal epithelial cells, glandular epithelial cells and stromal cells during the estrous cycle. In endometrial luminal epithelial cells, the hybridization signals for *Tgfa* mRNA did not appear to change, but the signals were higher in endometrial glandular epithelial cells at diestrus 1, 2 and proestrus. The number of stromal cells showing strong signals also appeared to increase at diestrus 1 and 2 (Fig. 2).

Effects of E2 and P4 on *Tgfa* mRNA expression in endometrial epithelial and stromal cells

To determine whether TGFα expression is regulated by

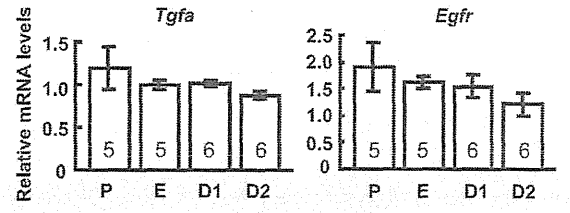

Fig. 1. Expression of *Tgfa* and *Egfr* mRNA in the mouse uterus during the estrous cycle. Uteri were obtained from adult female mice at each stage of the estrous cycle. Total RNA samples were extracted from the uterus, and real-time PCR analysis was performed using the specific primers listed in Table 1. Target mRNA levels were normalized according to *Rpl19* mRNA levels. Each column represents the mean ± SEM. The data are shown as relative values compared with that at proestrus. The number in each column indicates the number of mice used. P, proestrus; E, estrus; D1, 1st day of diestrus; D2, 2nd day of diestrus. Statistical analyses of *Tgfa* and *Egfr* mRNA levels during the estrous cycle were carried out using Steel-Dwass method, and significant differences were not detected.

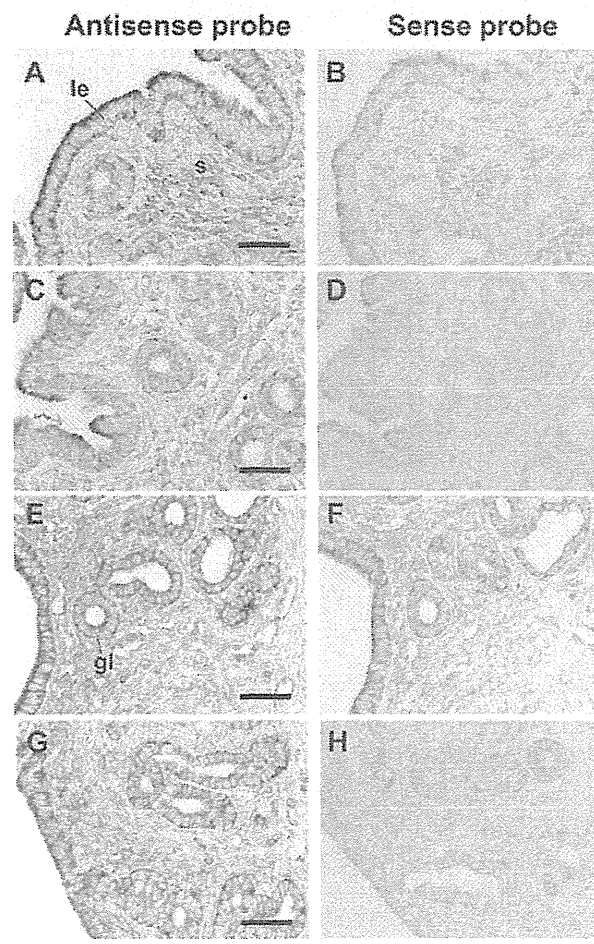

Fig. 2. In situ hybridization analysis of TGFα mRNA in the mouse uterus. Uteri were obtained from adult female mice at each stage of the estrous cycle (**(A, B)** proestrus, **(C, D)** estrus, **(E, F)** 1st day of diestrus, **(G, H)** 2nd day of diestrus). The uteri were sectioned and hybridized with biotin-16-UTP labeled antisense and sense probes. No strong signal was detected when the sense probe was used for hybridization (B, D, F, H). le, endometrial luminal epithelial cell; gl, endometrial glandular epithelial cell; s, endometrial stromal cell. Bar = 100 μm.

steroid hormones, we studied the effects of E2 and P4 treatment of *Tgfa* mRNA levels in vitro. The cultured endometrial cells were treated with E2 and/or P4 for 24 hr. Real-time PCR analysis revealed that *Tgfa* mRNA was expressed in both endometrial epithelial and stromal cells. E2 treatment increased *Tgfa* mRNA levels in endometrial stromal cells in a dose-dependent manner, but not in endometrial epithelial cells (Fig. 3A). P4 treatment also increased *Tgfa* mRNA levels in stromal cells in a dose dependent manner, but not in endometrial epithelial cells. Treatment with a combination of E2 (10^{-9}M) and P4 (10^{-7}M) decreased *Tgfa* mRNA levels in endometrial stromal cells compared with E2 or P4 alone (Fig. 3B).

Effects of E2, P4 and TGFα on DNA synthesis in endometrial stromal cells

The proliferation of endometrial stromal cells is stimulated by E2 and P4 treatment (Huet-Hudson et al., 1989; Komatsu et al., 2003), and TGFα treatment stimulated DNA synthesis in endometrial stromal cells (Komatsu et al., 2003). Therefore, the involvement of TGFα in E2 and P4-induced proliferation of stromal cells was studied. Endometrial stromal cells were treated with E2 (10^{-9}M), a combination of E2 and P4 (10^{-7}M), or TGFα (10 ng/ml) for 24 hr with or without anti-human TGFα antibody (10 μg/ml). DNA synthesis was measured by detecting BrdU incorporation in endometrial stromal cells (Fig. 4). E2 and P4 treatment, and TGFα treatment stimulated DNA synthesis in endometrial stromal cells. Anti-human TGFα antibody treatment inhibited the DNA-synthesizing effect of TGFα on endometrial stromal cells, but did not affect E2 and P4-induced DNA synthesis in endometrial stromal cells.

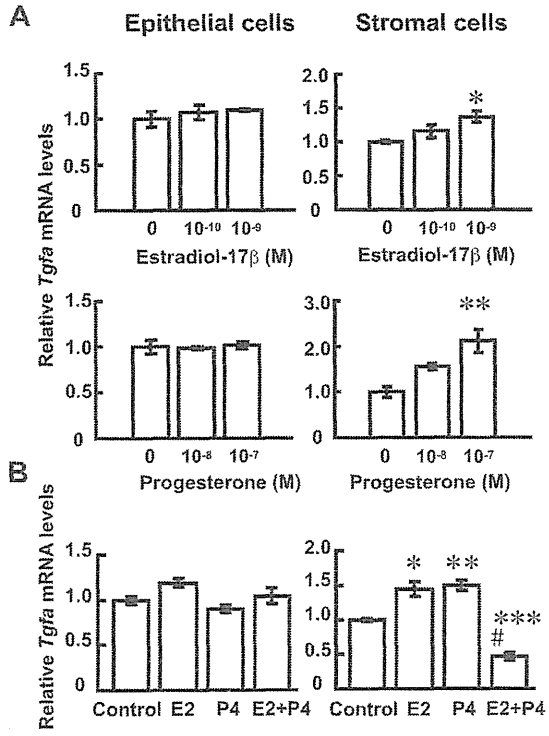

Fig. 3. Effect of E2 and P4 on *Tgfa* mRNA expression in endometrial cells. **(A)** Endometrial epithelial cells and stromal cells were treated with E2 (0, 10^{-10} and 10^{-9} M) or P4 (0, 10^{-8} and 10^{-7} M) for 24 hr. **(B)** Endometrial epithelial cells and stromal cells were treated with E2 (10^{-9} M) and/or P4 (10^{-7} M) for 24 hr. *Tgfa* mRNA levels were analyzed by Real-time PCR. Each column represents the mean ± SEM of three independent samples. *, $P < 0.05$, **, $P < 0.01$, ***, $P < 0.001$: significantly different from control; #, significantly different from E2 ($P < 0.01$) and P4 ($P < 0.001$).

Effects of TGFα on *Igf1*, *Igf1r* and *Igfbp3* mRNA expression in endometrial stromal cells

TGFα, in addition to E2 and P4, stimulated the prolifer-

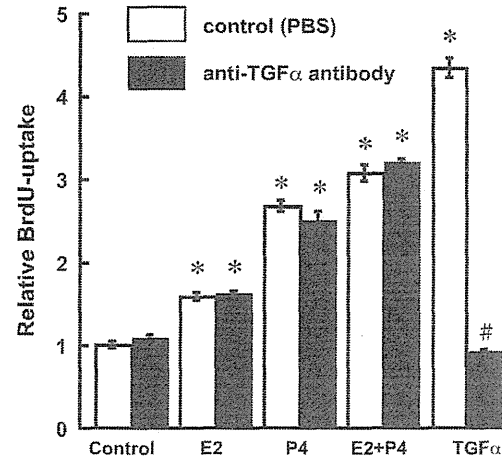

Fig. 4. Effects of E2, P4 and TGFα on DNA synthesis in cultured endometrial stromal cells. Endometrial stromal cells were treated with E2 (10^{-9} M), P4 (10^{-7} M) or TGFα (10 ng/ml) in the presence or absence of anti-human TGFα antibody (10 μg/ml) for 24 hr. BrdU (100 μM) was added for the last 2 hr of incubation. BrdU incorporation into the nucleus was analyzed in terms of DNA synthesis. Each column represents the mean ± SEM of triplicate wells. Experiments were repeated three times. *, $P < 0.001$: significantly different from the corresponding control; #, $P < 0.001$: significantly different from PBS treatment.

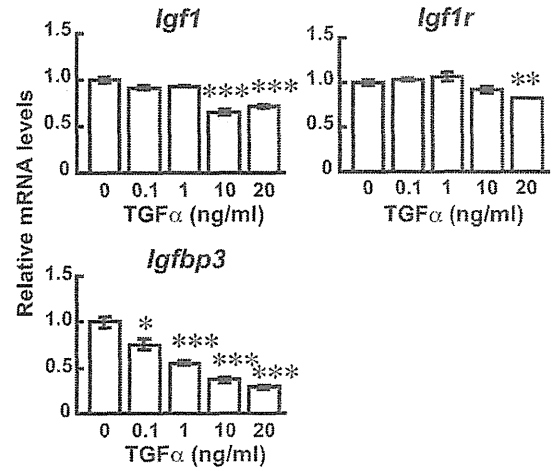

Fig. 5. Effect of TGFα on *Igf1*, *Igfbp3* and *Igf1r* mRNA expression in endometrial stromal cells. Endometrial stromal cells were treated with TGFα for 24 hr. *Igf1*, *Igfbp3* and *Igf1r* mRNA levels were analyzed by real-time PCR. Each column represents the mean ± SEM of triplicate wells. Experiments were repeated three times. *, $P < 0.05$; **, $P < 0.01$; ***, $P < 0.001$: significantly different from control.

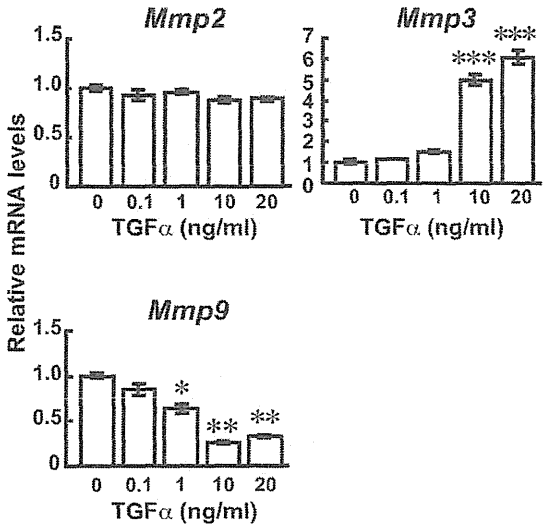

Fig. 6. Effect of TGFα on *Mmp2*, *Mmp3* and *Mmp9* mRNA expression in endometrial stromal cells. Endometrial stromal cells were treated with TGFα for 24 hr. *Mmp2*, *Mmp3* and *Mmp9* mRNA levels were analyzed by real-time PCR. Each column represents the mean ± SEM of triplicate wells. Experiments were replicated twice. *, $P < 0.01$; **, $P < 0.001$; ***, $P < 0.0001$: significantly different from control.

ation of endometrial stromal cells. To clarify the other roles of TGFα on endometrial cells, we studied the expression of the IGF family genes including *Igf1*, *Igf1r* and *Igfbp3*, because IGF1 is involved in the regulation of endometrial epithelial cells and stromal cells (Shiraga et al., 1997; Sato et al., 2002; Inoue et al., 2005; Maekawa et al., 2009). TGFα treatment decreased *Igfbp3* mRNA levels in a dose-dependent manner (Fig. 5). TGFα decreased *Igf1* and *Igf1r* mRNA levels at high doses (10 and 20 ng/ml, respectively).

Effects of TGFα on *Mmp2*, *Mmp3* and *Mmp9* mRNA expression in endometrial stromal cells

We examined the effects of TGFα on *Mmp2*, *Mmp3* and *Mmp9 mRNA* expression, because MMP activities are closely associated with the destruction of ECMs leading to changes in cell proliferation activity and cell mobility. *Mmp2*, *Mmp3* and *Mmp9 mRNA* levels were detected in cultured endometrial cells. TGFα treatment increased *Mmp3* mRNA levels (Fig. 6) and decreased *Mmp9* mRNA levels in a dose-dependent manner.

DISCUSSION

The present study demonstrated that *Tgfa* mRNA is expressed in three types of endometrial cells, namely, luminal epithelial cells, glandular epithelial cells and stromal cells, and that its expression varies during the estrous cycle. TGFα expression during pregnancy was previously reported. *Tgfa* mRNA and pro-TGFα are localized in luminal and glandular epithelium on days 1–4 of pregnancy and in many stromal cells on days 3 and 4 of pregnancy in the mouse uterus (Tamada et al., 1991; Paria et al., 1994). These findings suggest that TGFα is involved in the regulation of growth and differentiation of endometrium.

The effects of sex steroid hormones on *Tgfa* mRNA expression were analyzed using a primary cell culture system comprised of endometrial luminal epithelial and stromal cells. *Tgfa* mRNA expression in endometrial epithelial cells was not affected by E2 or P4, which is consistent with the results obtained with in situ hybridization that *Tgfa* mRNA levels did not appear to change during the estrous cycle. In contrast, E2 and P4 stimulated *Tgfa* mRNA expression in endometrial stromal cells, which is also consistent with the increased number of *Tgfa* mRNA-expressing cells at diestrus 1 and 2. Thus, *Tgfa* mRNA expression in the endometrium is regulated in a time- and tissue-specific manner.

In the mouse uterus, there are some reports of the mitogenic action of TGFα. Anti-rat TGFα antibody blocked the proliferation of epithelial cells induced by estrogen in the mouse uterus (Nelson et al., 1992). As expected, TGFα treatment increased DNA synthesis in endometrial epithelial and stromal cells. Similarly, E2 and P4 promoted the proliferation of endometrial stromal cells, and also stimulated *Tgfa* mRNA expression. From these results, we speculated that actions of steroid hormones on endometrial stromal cells were mediated by TGFα. However, the effects of steroid hormones were not inhibited with an anti-human TGFα antibody. It is not clear whether the anti-human TGFα antibody used in the present study can bind to membrane-anchored TGFα in the present culture system. Growth factors of the EGF family other than TGFα may be involved in the stimulation of endometrial growth as previously reported (Nelson et al., 1992; Komatsu et al., 2003).

The IGF1 system, which includes IGF1, IGFBP3 and the IGF receptor, plays a crucial role in the proliferation of endometrial cells. IGF1 stimulates DNA synthesis in endometrial epithelial and stromal cells (Shiraga et al., 1997; Inoue et al., 2005), and IGFBP3 inhibits IGF1-induced DNA synthesis in endometrial stromal cells (Maekawa et al., 2009). *Igfbp3* mRNA expression was detected by in situ hybridization in endometrial stromal cells in rats on the estrous morning (Girvigian et al., 1994) and in humans (Zhou et al., 1994). The present study revealed that *Igf1* mRNA expression was inhibited by a high dose of TGFα (10 ng/ml), suggesting that IGF1 alone cannot be a physiological mediator of TGFα-induced cell proliferation in the stroma. Low doses of TGFα (0.1 ng/ml) however decreased *Igfbp3* mRNA levels in endometrial stromal cells. This dose-dependency is comparable to be the effect of TGFα on stromal cell proliferation (Maekawa et al., 2009). Reduced *Igfbp3* transcription probably resulted in decreased IGFBP3 synthesis, leading to the enhanced availability of IGF1. Therefore, these results led us to the idea that TGFα indirectly regulates IGF1-induced endometrial cell proliferation through down-regulation of IGFBP3 synthesis. In fact, previous studies have shown that the production of IGFBP3 is partly regulated by members of the EGF (Hembree et al., 1994; Provenzano et al., 2005; Takaoka et al., 2006) and TGFβ families (Oh et al., 1995; Rajah et al., 1997; Cohen et al., 2000). The inhibitory effect of TGFα on *Igfbp3* mRNA expression is thought to be one of multiple regulatory mechanisms involved in the proliferation of endometrial cells.

MMPs are involved in reproductive functions through the degradation of ECM (Bruner et al., 1995; Singer et al., 1999; Nuttall and Kennedy, 2000b; Bunn and Fowlkes, 2003; Curry and Osteen, 2003; Gamo et al., 2007). We have demonstrated, for the first time, that TGFα increased *Mmp3*

mRNA levels and decreased *Mmp9* mRNA levels in endometrial stromal cells. *Mmp2* mRNA levels were not affected by TGFα treatment, which is consistent with a previous study showing that *Mmp2* mRNA expression in malignant mesothelioma cells was not affected by growth factors such as TGFα, EGF and IGF1 (Liu and Klominek, 2003). MMP3 and MMP9, stromelysin and gelatinase, can degrade the basement membrane, and MMP3 may be sufficient to degrade many types of ECM substrates. Importantly, MMP3 and MMP9 are known to degrade IGFBP3 (Fowlkes et al., 1994; Manes et al., 1999; Fowlkes et al., 2004). The degradation of IGFBP3 can increase the amount of free IGF1, thus enhancing IGF1 action, which may include the stimulation of cell proliferation. Thus, MMPs are involved in the degradation of ECM and IGFBP3, which is closely associated with the proliferation, mobility and differentiation of endometrial cells. These findings imply that TGFα, at a high dose (10 ng/ml), induces endometrial stromal cell proliferation not only through the inhibition of *Igfbp3* transcription but also through the stimulation of *Mmp3* transcription.

E2 or P4 induced *Tgfa* mRNA expression in endometrial stromal cells but not in endometrial epithelial cells. *Tgfa* mRNA levels from the whole uteri did not change throughout the estrous cycle, but in situ hybridization analysis showed that *Tgfa* mRNA signals were higher in glandular epithelial cells and stromal cells at diestrus 1 and 2. The present in vitro study using a primary culture system showed that endometrial luminal epithelial cells did not respond to E2 and P4, whereas endometrial stromal cells responded to E2 and P4. These findings correspond to changes in *Tgfa* mRNA signals revealed by the in situ hybridization analysis. The increase in *Tgfa* mRNA expression in endometrial stromal cells during the diestrous period was probably caused by progesterone secreted from the corpus luteum. A combined treatment of E2 and P4 decreased *Tgfa* mRNA levels. Concurrent increases in E2 and P4 levels occur at peri-implantation period. The tissue- and temporary-specific regulatory mechanisms of *Tgfa* transcription remain to be studied.

Recently, we found that *Igfbp3* mRNA expression in the endometrial stromal cells was inhibited by E2 (Maekawa et al., 2009), while *Igf1* mRNA expression in the uterus was stimulated by E2 (Murphy et al., 1987; Ghahary et al., 1990; Kapur et al., 1992; Ohtsuki et al., 2007). Thus, E2-induced changes not only in *Tgfa* and *Mmp3* mRNA expressions, but also in *Igf1* and *Igfbp3* mRNA expressions will give rise to increase the availability of IGF1, probably leading to the stimulation of cell proliferation in the endometrium.

In conclusion, *Tgfa* mRNA expression in endometrial stromal cells is positively regulated by E2 and P4. TGFα stimulated DNA synthesis in endometrial stromal cells, although it may not contribute to the stromal cell proliferation induced by these sex steroids. TGFα appeared to generate conditions favorable for the proliferation of endometrial stromal cells, partly by modifying the transcriptional activity of *Igfbp3*, *Mmp3* and *Mmp9*.

ACKNOWLEDGMENTS

This study was supported in part by a Grant-in-Aid-for Scientific Research from the Japan Society for the Promotion of Science to ST (No. 19370025). The authors declare that they have no conflict of interest that could be perceived as prejudicing the impartiality of the research reported.

REFERENCES

Aplin JD, Charlton AK, Ayad S (1988) An immunohistochemical study of human endometrial extracellular matrix during the menstrual cycle and first trimester of pregnancy. Cell Tissue Res 253: 231–240

Beck CA, Garner CW (1992) Stimulation of DNA synthesis in rat uterine cells by growth factors and uterine extracts. Mol Cell Endocrinol 84: 109–118

Bruner KL, Rodgers WH, Gold LI, Korc M, Hargrove JT, Matrisian LM, et al. (1995) Transforming growth factor beta mediates the progesterone suppression of an epithelial metalloproteinase by adjacent stroma in the human endometrium. Proc Natl Acad Sci USA 92: 7362–7366

Bunn RC, Fowlkes JL (2003) Insulin-like growth factor binding protein proteolysis. Trends Endocrinol Metab 14: 176–181

Chomczynski P, Sacchi N (1987) Single-step method of RNA isolation by acid guanidinium thiocyanate-phenol-chloroform extraction. Anal Biochem 162: 156–159

Cohen P, Nunn SE, Peehl DM (2000) Transforming growth factor-β induces growth inhibition and IGF-binding protein-3 production in prostatic stromal cells: abnormalities in cells cultured from benign prostatic hyperplasia tissues. J Endocrinol 164: 215–223

Cooke PS, Buchanan DL, Young P, Setiawan Y, Brody J, Korach KS, et al. (1997) Stromal estrogen receptors mediate mitogenic effects of estradiol on uterine epithelium. Proc Natl Acad Sci USA 94: 6535–6540

Curry TE, Jr, Osteen KG (2003) The matrix metalloproteinase system: changes, regulation, and impact throughout the ovarian and uterine reproductive cycle. Endocr Rev 24: 428–465

Das SK, Wang XN, Paria BC, Damm D, Abraham JA, Klagsbrun M, et al. (1994) Heparin-binding EGF-like growth factor gene is induced in the mouse uterus temporally by the blastocyst solely at the site of its apposition: a possible ligand for interaction with blastocyst EGF-receptor in implantation. Development 120: 1071–1083

DiAugustine RP, Petrusz P, Bell GI, Brown CF, Korach KS, McLachlan JA, et al. (1988) Influence of estrogens on mouse uterine epidermal growth factor precursor protein and messenger ribonucleic acid. Endocrinology 122: 2355–2363

Fowlkes JL, Suzuki K, Nagase H, Thrailkill KM (1994) Proteolysis of insulin-like growth factor binding protein-3 during rat pregnancy: a role for matrix metalloproteinases. Endocrinology 135: 2810–2813

Fowlkes JL, Serra DM, Bunn RC, Thrailkill KM, Enghild JJ, Nagase H (2004) Regulation of insulin-like growth factor (IGF)-I action by matrix metalloproteinase-3 involves selective disruption of IGF-I/IGF-binding protein-3 complexes. Endocrinology 145: 620–626

Gamo T, Yamauchi N, Nishimura K, Watanabe R, Matsumoto K, Oozono S, et al. (2007) Effects of tumor necrosis factor-α on cell proliferation, prostaglandins and matrix-metalloproteinases production in rat endometrial stromal cells cultured in vitro. J Exp Zool Part A Ecol Genet Physiol 307: 699–707

Ghahary A, Chakrabarti S, Murphy LJ (1990) Localization of the sites of synthesis and action of insulin-like growth factor-I in the rat uterus. Mol Endocrinol 4: 191–195

Giancotti FG, Ruoslahti E (1999) Integrin signaling. Science 285: 1028–1032

Girvigian MR, Nakatani A, Ling N, Shimasaki S, Erickson GF (1994) Insulin-like growth factor binding proteins show distinct patterns of expression in the rat uterus. Biol Reprod 51: 296–302

Hembree JR, Agarwal C, Eckert RL (1994) Epidermal growth factor suppresses insulin-like growth factor binding protein 3 levels in

human papillomavirus type 16-immortalized cervical epithelial cells and thereby potentiates the effects of insulin-like growth factor 1. Cancer Res 54: 3160–3166

Hotary KB, Allen ED, Brooks PC, Datta NS, Long MW, Weiss SJ (2003) Membrane type I matrix metalloproteinase usurps tumor growth control imposed by the three-dimensional extracellular matrix. Cell 114: 33–45

Huet-Hudson YM, Andrews GK, Dey SK (1989) Cell type-specific localization of *c-myc* protein in the mouse uterus: modulation by steroid hormones and analysis of the periimplantation period. Endocrinology 125: 1683–1690

Inoue A, Takeuchi S, Takahashi S (2005) Insulin-like growth factor-I stimulated DNA replication in mouse endometrial stromal cells. J Reprod Dev 51: 305–313

Itoh N, Patel U, Skinner MK (1998) Developmental and hormonal regulation of transforming growth factor-α and epidermal growth factor receptor gene expression in isolated prostatic epithelial and stromal cells. Endocrinology 139: 1369–1377

Iwahashi M, Ooshima A, Nakano R (1997) Effects of oestrogen on the extracellular matrix in the endometrium of postmenopausal women. J Clin Pathol 50: 755–759

Kapur S, Tamada H, Dey SK, Andrews GK (1992) Expression of insulin-like growth factor-I (IGF-I) and its receptor in the periimplantation mouse uterus, and cell-specific regulation of IGF-I gene expression by estradiol and progesterone. Biol Reprod 46: 208–219

Komatsu N, Maekawa T, Takeuchi S, Takahashi S (2003) Epidermal growth factor and transforming growth factor-α stimulate the proliferation of mouse uterine stromal cells. Zool Sci 20: 639–645

Liu Z, Klominek J (2003) Regulation of matrix metalloprotease activity in malignant mesothelioma cell lines by growth factors. Thorax 58: 198–203

Maekawa T, Takeuchi S, Kanayama M, Takahashi S (2009) Estradiol, progesterone, and transforming growth factor α regulate insulin-like growth factor binding protein-3 (IGFBP3) expression in mouse endometrial cells. Zool Sci 26: 131–138

Manes S, Llorente M, Lacalle RA, Gomez-Mouton C, Kremer L, Mira E, et al. (1999) The matrix metalloproteinase-9 regulates the insulin-like growth factor-triggered autocrine response in DU-145 carcinoma cells. J Biol Chem 274: 6935–6945

Murphy LJ, Bell GI, Friesen HG (1987) Tissue distribution of insulin-like growth factor I and II messenger ribonucleic acid in the adult rat. Endocrinology 120: 1279–1282

Nelson KG, Takahashi T, Lee DC, Luetteke NC, Bossert NL, Ross K, et al. (1992) Transforming growth factor-α is a potential mediator of estrogen action in the mouse uterus. Endocrinology 131: 1657–1664

Nuttall RK, Kennedy TG (2000) Epidermal growth factor and basic fibroblast growth factor increase the production of matrix mettaloproteinases during *in vitro* decidualization of rat endometrial stromal cells. Endocrinology 141: 629–636

Oh Y, Muller HL, Ng L, Rosenfeld RG (1995) Transforming growth factor-β-induced cell growth inhibition in human breast cancer cells is mediated through insulin-like growth factor-binding protein-3 action. J Biol Chem 270: 13589–13592

Ohtsuki T, Otsuki M, Murakami Y, Hirata K, Takeuchi S, Takahashi S (2007) Alternative leader-exon usage in mouse IGF-I mRNA variants: class 1 and class 2 IGF-I mRNAs. Zool Sci 24: 241–247

Paria BC, Das SK, Huet-Hudson YM, Dey SK (1994) Distribution of transforming growth factor α precursors in the mouse uterus during the periimplantation period and after steroid hormone treatments. Biol Reprod 50: 481–491

Provenzano AP, Besner GE, James PF, Harding PA (2005) Heparin-binding EGF-like growth factor (HB-EGF) overexpression in transgenic mice downregulates insulin-like growth factor binding protein (IGFBP)-3 and -4 mRNA. Growth Factors 23: 19–31

Rajah R, Valentinis B, Cohen P (1997) Insulin-like growth factor (IGF)-binding protein-3 induces apoptosis and mediates the effects of transforming growth factor-β1 on programmed cell death through a p53- and IGF-independent mechanism. J Biol Chem 272: 12181–12188

Reddy KB, Yee D, Hilsenbeck SG, Coffey RJ, Osborne CK (1994) Inhibition of estrogen-induced breast cancer cell proliferation by reduction in autocrine transforming growth factor α expression. Cell Growth Differ 5: 1275–1282

Ross AK, Nelson KG, Sakai Y, Fukamachi H, Burroughs CD, McLachlan JA (1993) Isolation and culture of mouse uterine epithelial and stromal cells. In "Methods in Toxicology" Ed by JJ Heindel, RE Chapin, Academic Press, Inc., San Diego, pp 371–385

Russo LA, Peano BJ, Trivedi SP, Cavalcanto TD, Olenchock BA, Caruso JA, et al. (2009) Regulated expression of matrix metalloproteinases, inflammatory mediators, and endometrial matrix remodeling by 17β-estradiol in the immature rat uterus. Reprod Biol Endocrinol 7: 124

Sato T, Wang G, Hardy MP, Kurita T, Cunha GR, Cooke PS (2002) Role of systemic and local IGF-I in the effects of estrogen on growth and epithelial proliferation of mouse uterus. Endocrinology 143: 2673–2679

Sharma S, Oomizu S, Kakeya T, Masui T, Takeuchi S, Takahashi S (2003) Gene expression and the physiological role of transforming growth factor-α in the mouse pituitary. Zool Sci 20: 83–89

Shiraga M, Takahashi S, Miyake T, Takeuchi S, Fukamachi H (1997) Insulin-like growth factor-I stimulates proliferation of mouse uterine epithelial cells in primary culture. Proc Soc Expl Biol Med 215: 412–417

Singer CF, Marbaix E, Lemoine P, Courtoy PJ, Eeckhout Y (1999) Local cytokines induce differential expression of matrix metalloproteinases but not their tissue inhibitors in human endometrial fibroblasts. Eur J Biochem 259: 40–45

Taga M, Sakakibara H, Suyama K, Ikeda M, Minaguchi H (1997) Gene expression of transforming growth factor-α in human endometrium during decidualization. J Assist Reprod Genet 14: 218–222

Takaoka M, Smith CE, Mashiba MK, Okawa T, Andl CD, El-Deiry WS, et al. (2006) EGF-mediated regulation of IGFBP-3 determines esophageal epithelial cellular response to IGF-I. Am J Physiol Gastrointest Liver Physiol 290: G404–416

Tamada H, Das SK, Andrews GK, Dey SK (1991) Cell-type-specific expression of transforming growth factor-α in the mouse uterus during the peri-implantation period. Biol Reprod 45: 365–372

Tamada H, Sakaguchi H, Inaba T, Kawate N, Sawada T (2001) The effect of transforming growth factor-α on the progression of decidualization in rats. Life Sci 69: 1549–1558

Tomooka Y, DiAugustine RP, McLachlan JA (1986) Proliferation of mouse uterine epithelial cells in vitro. Endocrinology 118: 1011–1018

Weiser M, Baker H, Wessel TC, Joh TH (1993) Differential spatial and temporal gene expression in response to axotomy and deafferentation following transection of the medial forebrain bundle. J Neurosci 13: 3472–3484

Zhou J, Dsupin B, Giudice L, Bondy C (1994) Insulin-like growth factor system gene expression in human endometrium during the menstrual cycle. J Clin Endocrinol Metab 79: 1723–1734

Zhu L, Pollard JW (2007) Estradiol-17β regulates mouse uterine epithelial cell proliferation through insulin-like growth factor 1 signaling. Proc Natl Acad Sci USA 104: 15847–15851

(Received November 17, 2011 / Accepted January 17, 2012)

Cell Tissue Res (2012) 348:239–247
DOI 10.1007/s00441-012-1350-7

REGULAR ARTICLE

Hedgehog signaling plays roles in epithelial cell proliferation in neonatal mouse uterus and vagina

Tadaaki Nakajima · Taisen Iguchi · Tomomi Sato

Received: 27 November 2011 / Accepted: 20 January 2012 / Published online: 3 March 2012

Abstract Both the uterus and vagina develop from the Müllerian duct but are quite distinct in morphology and function. To investigate factors controlling epithelial differentiation and cell proliferation in neonatal uterus and vagina, we focused on Hedgehog (HH) signaling. In neonatal mice, Sonic hh (*Shh*) was localized in the vaginal epithelium and Indian hh (*Ihh*) was slightly expressed in the uterus and vagina, whereas all Glioma-associated oncogene homolog (*Gli*) genes were mainly expressed in the stroma. The expression of target genes of HH signaling was high in the neonatal vagina and in the uterus, it increased with growth. Thus, in neonatal mice, *Shh* in the vaginal epithelium and *Ihh* in the uterus and vagina activated HH signaling in the stroma. Tissue recombinants showed that vaginal *Shh* expression was inhibited by the vaginal stroma and uterine *Ihh* expression was stimulated by the uterine stroma. Addition of a HH signaling inhibitor decreased epithelial cell proliferation in organ-cultured uterus and vagina and increased stromal cell proliferation in organ-cultured uterus. However, it did not affect epithelial differentiation or the expression of growth factors in organ-cultured uterus and vagina. Thus, activated HH signaling stimulates epithelial cell proliferation in neonatal uterus and vagina but inhibits stromal cell proliferation in neonatal uterus.

Keywords Hedgehog · Uterus · Vagina · Cell proliferation · Organ culture · Mouse (female C57BL/6J)

Introduction

Female reproductive tracts originate from the Müllerian duct. The middle to upper portion of the Müllerian duct develops into the oviduct and uterus and the lower portion, which is connected to the urogenital sinus, develops into the vagina in embryonic and neonatal mice. Kurita (2010) has shown that the Müllerian vagina extends to the caudal end of the body by day 8, suggesting that, in adults, both the uterus and vagina have developed from the Müllerian duct. However, the uterus and vagina are quite distinct in their morphology and function. The uterine epithelium (UE) is composed of a simple columnar luminal epithelium and a glandular epithelium. The Müllerian vaginal epithelium (VE) consisting in pseudostratified columnar cells develops into a stratified cuboidal epithelium with markers of stratification, namely transformation related protein 63 (TRP63) and keratin 14 (KRT14) expression (Forsberg 1965; Nakajima et al. 2011). *Trp63* is necessary for differentiation into stratified squamous epithelium since, in *Trp63* knockout mice, the

Electronic supplementary material The online version of this article (doi:10.1007/s00441-012-1350-7) contains supplementary material, which is available to authorized users.

This work was partially supported by a Grant-in-Aid for Scientific Research (B) to T.I. from the Ministry of Education, Culture, Sports, Science and Technology of Japan, Grants for Strategic Research Projects at Yokohama City University (nos. K19020, K2109, G2201 and W18005 to T.S.), a Health Sciences Research Grant from the Ministry of Health, Labor and Welfare, Japan (to T.I.) and a Grant for Support of the Collaborative Study at NIBB (to T.S). T.N. is a Research Fellow of the Japan Society for the Promotion of Science.

The authors declare no conflicts of interest.

T. Nakajima · T. Sato (✉)
Graduate School of Nanobioscience, Yokohama City University, Yokohama 236-0027, Japan
e-mail: tomomi@yokohama-cu.ac.jp

T. Iguchi
The Graduate University for Advanced Studies and Okazaki Institute for Integrative Bioscience, National Institute for Basic Biology, National Institutes of Natural Sciences, Okazaki 444-8787, Japan

Müllerian VE forms a uterus-like single layer of columnar epithelium (Kurita et al. 2004).

Tissue recombination of the epithelium and stroma has been performed in order to investigate the mechanism of epithelial differentiation from the Müllerian duct. The UE combined with the vaginal stroma (VS) of neonatal mice differentiates from a simple columnar epithelium into a TRP63- and KRT14-positive stratified squamous epithelium (Cunha 1976; Kurita et al. 2004; Nakajima et al. 2011). Similarly, the VE combined with the uterine stroma (US) shows a TRP63- and KRT14-negative single layer of columnar cells typical of the UE. These data indicate that epithelial-stromal signaling decides epithelial fate, differentiation and growth in the female reproductive tracts of developing mice. This epithelial cell differentiation in the uterus and vagina can be induced by the mesenchyme up to day 7 (Cunha 1976), suggesting that epithelial cell differentiation in the uterus and vagina is completed around day 7.

The Hedgehog (HH) family has been well studied as one of the paracrine regulators in epithelial-stromal interactions in developing intestine, limb, lung and prostate (Pepicelli et al. 1998; van Tuyl and Post 2000; Ramalho–Santos et al. 2000; McMahon et al. 2003; Madison et al. 2005; White et al. 2006; Jiang and Hui 2008). The HH family includes Sonic HH (SHH), Indian HH (IHH) and Desert HH (DHH). Binding of a HH ligand to a transmembrane receptor, namely patched 1 (PTCH1) or PTCH2, relieves the transmembrane protein called smoothened (SMO) and HH signaling is then activated through the transcription factors, Glioma-associated oncogene homolog 1 (GLI1) and GLI2 (Cohen 2003; Shaw and Bushman 2007). GLI3 is known as a transcriptional repressor balancing and refining GLI1 and GLI2 activation. The mRNA expression of *Gli1* and *Ptch1* increases in response to HH signaling activation and therefore, those genes are useful as markers of HH signaling activation.

In the developing prostate, *Shh* is localized in the epithelium, whereas *Gli1*, *Ptch1* and *Ptch2* are localized in the stroma (Lamm et al. 2002). In the organ-cultured developing prostate, the addition of SHH decreases the number of ductal tips, epithelial cell proliferation and TRP63-positive basal cells, whereas these parameters are increased by the HH signaling inhibitor, cyclopamine (Freestone et al. 2003; Wang et al. 2003; Berman et al. 2004). Loss-of-function in *Gli2* increases the number of TRP63-positive basal cells (Doles et al. 2006). These data indicate that epithelial SHH activates HH signaling in the stroma and then inhibits epithelial differentiation and cell proliferation in the developing prostate. However, Lamm et al. (2002) have shown that HH signaling in the developing prostate stimulates epithelial cell proliferation. Thus, the role of HH signaling in epithelial cell proliferation and ductal morphogenesis is complicated and seems to depend on the developmental stage (Vezina and Bushman 2007). In addition, epithelial SHH stimulates the stromal expression of transforming growth factor β1 (*Tgfβ1*), bone morphogenetic protein 4 (*Bmp4*) and *activin βA-subunit* and inhibits the stromal expression of fibroblast growth factor 10 (*Fgf10*) in the developing prostate, suggesting that activated HH signaling in the stroma can affect the epithelium through the regulation of the expression of these genes (Wang et al. 2003; Pu et al. 2004).

In the uterus, constitutive activation of SMO causes the epithelium to contain vagina-like stratified cells in adults and wingless-related MMTV integration site 5a (*Wnt5a*) expression is stimulated at day 24 (Franco et al. 2010a; Migone et al. 2011). Thus, HH signaling regulates epithelial differentiation in the immature and adult uterus. However, the role of HH signaling in the neonatal mouse uterus and vagina has not yet been investigated. In order to investigate epithelial differentiation and cell proliferation in the female reproductive tracts of neonatal mice, we have examined the ontogenic mRNA expression and localization of genes related to HH signaling in the uterus and vagina and the effects of cyclopamine on epithelial differentiation and cell proliferation in the uterus and vagina grown *in vitro*. Furthermore, in order to investigate the epithelial-stromal interactions, the mRNA expression of the *Shh* and *Ihh* has also been examined in the tissue recombinant.

Materials and methods

Animals

Female C57BL/6J mice (CLEA, Tokyo, Japan) were given a commercial diet (MF, Oriental Yeast, Tokyo, Japan) and tap water *ad libitum* and were kept at 22±1.0°C under a 12 h light/12 h darkness regime in artificial illumination (lights on: 0800–2000). Animals were maintained in accordance with the NIH Guide for the Care and Use of Laboratory Animals approved by our Institutional Animal Care Committee. Uteri and vaginae of 0- and 2-day-old mice containing undifferentiated epithelium and those of 15-day-old mice containing differentiated epithelium were examined.

Mice were ovariectomized at day 90. At 7 days after surgery, ovariectomized mice were given a single subcutaneous injection containing 0.1 μg/25 g body weight of 17β-estradiol (E2, Sigma, St. Louis, MO, USA) dissolved in sesame oil or sesame oil alone. At 16 h after a single injection of E2, vaginae were collected for real-time reverse transcription with the polymerase chain reaction (RT-PCR).

Epithelial-stromal separation, tissue recombination, and grafting

Epithelial-stromal separation, tissue recombination and grafting were performed as described previously (Bigsby et al. 1986; Nakajima et al. 2011). Uteri and vaginae of 2- and 15-day-old

mice were cut, placed into 1% trypsin (Becton, Dickinson, Franklin Lakes, NJ, USA) in Hanks' balanced salt solution (HBSS; Sigma) and digested at 4°C for 90 min. Trypsin action was stopped by addition of fetal bovine serum (FBS; Invitrogen, Carlsbad, CA, USA). UE, US, VE and VS were separated mechanically by using fine surgical forceps, immediately frozen in liquid nitrogen and stored at -80°C for RT-PCR.

For tissue recombination, UE recombined with US (UE+US) or VS (UE+VS) or VE recombined with VS (VE+VS) or US (VE+US) from 2-day-old mice were placed on agar plates and allowed to adhere at 37°C in a 5% CO_2 atmosphere overnight. Tissue recombinants were grafted under the renal capsules of 60- to 90-day-old C57BL/6J mice. At the time of grafting, all host mice were ovariectomized. They were then killed to harvest tissue recombinants at days 5 and 7 post-grafting, because transition from the UE to the VE and *vice versa* in tissue recombinants was completed at day 7 post-grafting (Nakajima et al. 2011). These tissue recombinants were placed immediately in liquid nitrogen and stored at -80°C for real-time RT-PCR.

Organ culture system

An organ culture system for neonatal uterus and vagina was modified according to previous reports (Ootani et al. 2009; Nakajima et al. 2011). Eight volumes of Cellmatrix type I-A (Nitta Gelatin, Osaka, Japan) were mixed with 1 volume 10× Dulbecco's Modified Eagle's Medium/Nutrient Mixture Ham's F-12 (DMEM/F12; Sigma) and then 1 volume 200 mM HEPES buffer containing 262 mM $NaHCO_3$ and 0.05 N NaOH was added to the mixture. This cold gelation mixture (200 μl) was poured into inner millicell cell culture inserts (Millipore, Bedford, Mass., USA) placed into the well of a 24-well plate and allowed to gel at 37°C. Uteri and vaginae of 0-day-old mice were cut and placed into HBSS. Tissues were washed three times in HBSS and mixed with fresh 200 μl cold gelation mixture. Tissues and gelation mixture were overlaid onto a base of gelled collagen in each cell culture insert and allowed to gel at 37°C. Subsequently, 200 μl 20% FBS in DMEM/F12 (Invitrogen) was added to each well and tissues were cultured at 37°C in a humidified, 5% CO_2/air atmosphere for 2 or 5 days. Medium was changed at day 3 of culture. Cyclopamine (10 μM; Enzo Life Sciences, Farmingdale, NY, USA) was added to the medium from day 0 of culture (Freestone et al. 2003; Wang et al. 2003; Berman et al. 2004). For immunohistochemistry of 5-bromo-2′-deoxyuridine (BrdU), uteri and vaginae were cultured with 18% FBS in DMEM/F12 containing 0.1 mg/ml BrdU (Sigma) for 2 h before fixation.

Immunohistochemistry of TRP63, KRT14 and BrdU

Immunohistochemistry of TRP63, KRT14 and BrdU was performed on organ-cultured uteri and vaginae. For TRP63 and KRT14, samples (n=7) were fixed in 4% paraformaldehyde in phosphate-buffered saline (pH 7.4) at 4°C, whereas BrdU samples (n=7–10) were fixed in 10% formalin neutral buffered solution (Wako Pure Chemical Industries, Osaka, Japan), both as described previously (Kim et al. 2009; Nakajima et al. 2011). Hematoxylin was used for counterstaining. Cells immunoreactive for BrdU were counted under a light microscope with a 40× objective lens. BrdU-positive cells were counted randomly in 600 cells in each of the UE, US, VE and VS.

RNA isolation and RT-PCR

UE, US, VE and VS of 2- and 15-day-old mice were homogenized in TRIzol (Invitrogen). Total RNA was purified by using an RNeasy total RNA kit (Qiagen, Hilden, Germany) and reverse-transcribed into cDNA. To determine the expression of *Shh*, *Ihh*, *Dhh*, *Ptch1*, *Ptch2*, *Gli1*, *Gli2*, *Gli3*, *Krt8*, or *vimentin*, an aliquot of cDNA was amplified with specific primers (see Supplemental Table) derived from mouse mRNA sequences. Reverse transcription and PCR were carried out by using the Takara RNA PCR Kit (AMV; Takara Bio, Otsu, Japan). Peptidylprolyl isomerase A (*Ppia*) was chosen as an internal standard. Ten UE, US, VE and VS of 2-day-old mice and two UE, US, VE and VS of 15-day-old mice were pooled for RNA isolation at each point. Two independent experiments were carried out for each study.

Real-time RT-PCR

Real-time RT-PCR was preformed as described previously (Nakajima et al. 2011). Total RNA was isolated from uteri and vaginae of 2- or 15-day-old mice, vaginae of oil- or E2-treated 90-day-old mice and UE+US, UE+VS, VE+VS and VE+US tissue recombinants at days 5 or 7 post-grafting and from organ-cultured uteri and vaginae for 2 or 5 days. To determine the expression of *Shh*, *Ihh*, *Dhh*, *Gli1*, *Gli2*, *Gli3*, *Ptch1*, *Ptch2*, *Tgf1*, *Bmp4*, *activin βA-* or *βB-subunit*, *Fgf7*, *Fgf10*, or *Wnt5a*, an aliquot of cDNA was amplified with specific primers (see Supplemental Table) derived from mouse mRNA sequences. *Ppia* was chosen as an internal standard. Twelve uteri and vaginae of 2-day-old mice, four uteri and vaginae of 15-day-old mice, a vagina of a 90-day-old mouse, a tissue recombinant at days 5 or 7 of post-grafting and five organ-cultured tissues were pooled for RNA isolation at each point. Three to seven independent experiments were carried out.

Statistical analyses

Data are expressed as means±SE. Differences were estimated by using an analysis of variance followed by appropriate *post hoc* tests. A two-tailed Student's t-test or Welch's t-test was used for the comparison of two means. Differences were considered significant at $P<0.05$.